Isotopic insights into the dynamics of soil water pools along an elevation gradient

Jiri Kocum[1,2], Kristyna Falatkova[1], Vaclav Sipek[1], Karel Patek[1,3], Jan Haidl[1], Ondrej Gebousky[1], Jan Hnilica[1], Michal Jenicek[2], Martin Sanda[4], Lukas Trakal[5], and Lukas Vlcek[1]

[1] Institute of ~~Hydrodynamics~~ Hydrology of the Czech Academy of Sciences, Prague, 160 00, Czech Republic
[2] Department of Physical Geography and Geoecology, Faculty of Science, Charles University, Prague, 128 00, Czech Republic
[3] Department of Water Resources and Environmental Modeling, Faculty of Environmental Sciences, Czech University of Life Sciences, Prague, 165 00, Czech Republic
[4] Department of Landscape Water Conservation, Faculty of Civil Engineering, Czech Technical University in Prague, Prague, 166 29, Czech Republic
[5] Department of Environmental Geosciences, Faculty of Environmental Sciences, Czech University of Life Sciences, Prague, 165 00, Czech Republic

Correspondence to: Jiri Kocum (kocum@ih.cas.cz)

Abstract. Recent intensive research on the soil–plant–atmosphere continuum has introduced novel methodological approaches. These include new in-situ extraction techniques and the application of stable hydrogen and oxygen isotopes in ~~-~~water enabling to trace water movement and plant responses at much finer spatial and temporal scales. Such approaches provide detailed insights into soil water dynamics and plant adaptation to changing environmental conditions under climate change. This study aims to provide a~~at an intimate~~ comprehensive ~~description~~ characterization of dynamics of distinct soil water pools—mobile versus tightly bound water—along an elevation gradient, while simultaneously assessing~~parallelly with an~~ the impact of the absen~~tee of~~ snow accumulation in lowland areas on soil water distribution ~~within the soil profile~~ compared to higher elevations. In contrast to conventional bulk water sampling, a ~~-~~key innovation of this study~~research~~ lies in the experimental design across the elevation gradient combined with~~and employing~~ a novel extraction method that selectively isolates tightly bound soil water for isotopic analysis. The ~~Our~~ results indicate a prolonged residence time of winter-derived soil water in lowland sites~~, despite limited snow cover~~, in contrast~~ing~~ to a rapid turnover at the highest elevation, where the winter water signal dissipate~~d~~ shortly after snowmelt. D~~Simultaneously, d~~istinct isotopic compositions among water pools—mobile versus tightly bound water—were particularly evident~~also~~ ~~found, especially~~ in lowland areas at the edges of the growing season (up to 3 ‰ and 21 ‰ for $\delta^{18}O$ and $\delta^{2}H$, respectively), while tightly bound and bulk soil water exhibited—on average—only minor or no isotopic differences. In~~Facing~~ the context of the projected continued decline in snow cover at higher elevations in Central Europe, these findings are ~~-~~critical for improving predictions of soil water storage and, consequently, plant water availability under ongoing climate change.

1 Introduction

Soil drought is becoming increasingly prevalent due to climate change, which alters air temperature, total amount of precipitation and its intra-annual distribution (Gebrechorkos et al., 2025; Samaniego et al., 2018). These shifts have contributed to a sustained decline in vegetation-accessible water over the past three decades (Jiao et al., 2021). In response, there has been growing interest in the role of snowpack water storage and runoff generation in snow-dominated catchments, which are essential for groundwater recharge and soil moisture replenishment (Jenicek et al., 2020, 2021; Šípek et al., 2021; Musselman et al., 2017). Numerous studies project a continued decline in snow cover across mountainous regions as a consequence of rising air temperatures (Musselman et al., 2017; Marty et al., 2017; Jenicek et al., 2018; Willibald et al., 2020), accompanied by a shift from snowfall to rainfall during the winter season (Harpold et al., 2017; Safeeq et al., 2016). The ~~implications~~ impacts of these changes on~~in~~ snow storage for the annual water balance represent~~main~~ a critical and unresolved question in hydrological research. Equally important issues are the downstream consequences for plant-available water in lowland ecosystems, particularly during the latte~~r~~ part of the growing season when drought stress is most acute (Büntgen et al., 2021; Qin et al., 2020; Mankin et al., 2019). A thorough~~comprehensive~~ understanding of the soil–plant–atmosphere continuum, a concept originally introduced by Gradmann (1928) and later formalized by van den Honert (1948), is therefore crucial for predicting vegetation dynamics and adaptive responses under increasingly frequent and severe drought periods~~conditions~~.

The relationship between plant water use and local hydrology has been studied since the early 20th century (Bates et al., 1921). Pioneering studies on water transport through soils and plants were ~~subsequently~~ summarized in comprehensive reviews (e.g., Tinker, 1976; Weatherley, 1976; Molz, 1981). A major shift in perspective occurred when Dawson and Ehleringer (1991) demonstrated that some riparian trees primarily access deeper groundwater, rather than the more readily available stream water. ~~However, later work by~~A decade later, Bond et al. (2002) appeared to challenge this finding by demonstrating diel fluctuations in stream baseflow attributable to plant transpiration, demonstrating clear interactions between transpiration and streamflow. Despite this apparent contradiction, Brooks et al. (2010) showed that mobile ~~water (represented by stream water)~~ and tightly bound soil water (represented by the stream and plant water, respectively) are isotopically distinct. Their results suggested that, especially during the dry season, mobile water traveling through macropores or pipes bypasses tightly bound soil water, which is instead more likely to be taken up by plants and not contribute to streamflow.

This conceptual breakthrough formed the basis for the ecohydrological separation framework, later termed the “Two Water Worlds” (TWW) hypothesis (McDo~~n~~nell, 2014). Since then, the TWW hypothesis has stimulated widespread debate, with numerous studies supporting (e.g., Goldsmith et al., 2012; Evaristo et al., 2015; Hervé-Fernandez et al., 2016) or challenging (e.g., Geris et al., 2015; Vargas et al., 2017; Dubbert et al., 2019) the existence of isotopically distinct water pools for vegetation use and runoff generation. These contrasting findings prove, that ~~Despite ongoing refinements,~~ the hydrological connectivity between plant-accessible water and mobile water remains a central, unresolved question in ecohydrology and an issue of potential methodological and conceptual limitations in current approaches. Consequently, ~~.~~

~~Due to inconsistencies in the aforementioned studies,~~ a new way forward has been proposed (Berry et al., 2017), emphasizing the need to ~~. Key priorities for future research include~~ investigat~~e~~ing internal water cycling within the phloem and xylem, identifying potential sampling and methodological biases, and improv~~e~~ing both the spatial and temporal resolution of sampling strategies. ~~Dubbert et al. (2019) further highlight the need to develop a standardized sampling protocol to harmonize methodologies across research groups and thus improve the comparability of results. Such a protocol has recently been proposed by Ceperley et al. (2024).~~

However, an overwhelming ~~the vast~~ majority of studies comparing soil water and xylem water (e.~~-~~g., Zapater et al., 2011; Meunier et al., 2017; Vargas et al., 2017; Barbeta et al., 2019, 2020; Liu et al., 2021; Brighenti et al., 2024; Benettin et al., 2024) rely on mobile and so-called bulk soil water ~~for comparison~~to be compared. Mobile water is typically extracted using suction lysimeters or other vacuum-based systems. The water obtained in this manner—usually under tension of -60 kPa (Brooks et al., 2010; Muñoz-Villers and McDonnell, 2012; Berry et al., 2017; Sprenger et al. 2018; Haagsma et al., 2024)—originates primarily from macropores and preferential flow paths. In contrast, bulk soil water encompasses the total soil water content, including both gravitational and capillary pore water. During dry periods, when macropores are emptied and suction lysimeters cannot collect water, bulk soil water reliably represents the tightly bound water fraction. However, during wet ~~conditions~~periods, when gravitational pores are partially or fully saturated, a significant portion of the bulk soil water may also consist of mobile water. ~~Under such circumstances~~In this case, bulk water may no longer ~~serve as a representative of~~represent the tightly bound fraction and may not be as suitable for direct comparison with xylem water, particularly under the assumption that plants preferentially utilize tightly bound soil water (McDonell, 2014). In our study, mobile water (MW) and tightly bound water (TBW) are defined consistently with previous work mentioned above: MW is extracted at -60 kPa, while TBW is defined as the soil water remaining after the removal of MW. Bulk water (BW) is considered to represent the total soil water content.

The aim of this~~is~~ study is therefore to determine a~~investigated t~~ he distinction between mobile soil water and experimentally extracted ~~tightly bound soil water (~~TBW~~)~~, which is mostly examined only as a component of BW. ~~and mobile soil water (MW).~~ We hypothesize that ~~The~~ TBW differs in its isotopic composition from both MW and BW, and that this distinction persists for longer periods at higher elevations characterized by greater snow accumulation.~~, extracted using a novel experimental approach, was further compared with the potential composition of bulk soil water (BW) to assess whether these two components can be used interchangeably without significant differences in their isotopic composition.~~ To test this~~he~~ hypotheses, the experiments were~~as~~ conducted simultaneously at four sites spanning an elevation gradient ~~of more than~~exceeding 1000 meters. This~~e~~ elevation-focused design ~~on different elevations~~ is particularly relevant ~~especially important~~ in ~~areas in~~ the rain-snow transition zone, which ~~are~~ is highly sensitive~~widely affected by changes in snow storage due~~ to ~~increasing air~~ temperature-driven changes in snow storage. A s~~The s~~ite selection was considered ~~aimed~~ to locations with ~~capture the influence of declining snow cover and duration and reduced total precipitation on the isotopic behaviour of soil water. For this purpose, sites with~~ similar soil texture, given its strong influence on the relative abundance ~~were chosen, as soil texture strongly affects the proportion~~ of macropores and capillary pores. Soil water ~~The~~ sampling ~~campaign~~ was carried

outonducted at two-week intervals from February to November 2023, except at the highest--elevation site, which was accessible only from May onwards.

-The primary objectives of the study arewere to:

a. dDetermine whether tightly bound and mobile soil water there is a significant differ significantlyence in their isotopic composition;- of tightly bound and mobile soil water

b. characterizeEvaluate the dynamics- annual course of the isotopic composition of the soil water along the elevation gradient in relation to declining snow cover and overall precipitation;of soil water across the elevation gradient with regard to the decrease in snow cover and precipitation in general

c. iIdentify the dominant sources of tightly bound soil water; and

d. assessDetermine whether substitutingreplacing bulk soil water with tightly bound soil water alterscan lead to different resultsinterpretations of soil water sources and their seasonal dynamics.

2 Study sites

The experiment was conducted in Czechia at four experimental plots (Tab. 1 and Fig. 1) strategically selected to span a pronounced considerable elevation gradient covering , thereby capturing corresponding variations in temperature, precipitation, and snow cover extent and duration (Fig. 1). The study sites ranged from the fertile agricultural lowlands of the Elbe River Basin—Zvěřínek (185 m a.s.l.)—through the highlands and foothills—Trhové Dušníky (430 m a.s.l.) and the Liz catchment (870 m a.s.l.)—to the upper montane zone of the Bohemian Forest—Rokytka catchment (1,260 m a.s.l.). Throughout the manuscriptFor simplicity, these locations are referred to by the abbreviations ZV, TD, LI, and RO, respectively.

Although the soil types varyried due to the natural pedogenetic context of each site (Regosol, Gleyc Fluvisol, Cambisol, and Podzol), all plots exhibited similar soil texture (loamy sand or sandy loam). Thcis minimalmized confounding effects from differences in clay content provide , allowing for a more direct assessment of elevation-related influences on soil water behaviour. Owing Due to the considerablepronounced elevation differences, it was not feasible possible to maintain identical vegetation cover across all sites. However, vegetation at each location was representsative of typical plant communities found at the corresponding elevation zones in Central Europe—ranging from agricultural land in the lowlands, to meadows, spruce forest, and beech forest at higher elevations. The agricultural land at the lowest elevation (ZV) lacked vegetation cover from February to March, with post-harvest stubble remaining from October onward.

Table 1. Detailed characteristics of selected experimental areas. Climatic data (total annual precipitation and mean annual temperature) are for 2023. Snow data and climate classification (Köppen system) follow Tolasz et al. (2007). Further details for individual locations are provided in the cited references.

Name of the location	Zvěřínek (ZV)	Trhové Dušníky (TD)	Liz (LI)	Rokytka (RO)

Coordinates		50° 9' 20" N 15° 0' 37" E	49° 43' 12" N 14° 0' 46" E		49° 4' 0.2" N 13° 40' 49" E		49° 1' 22" N 13° 24' 23" E	
Elevation (m a. s. l.)		185	430		870		1,260	
Total precipitation (mm year^{-1})		631	680		931		1,380	
Average annual temperature (°C)		9.2	7		6.7		4.8	
Max snow depth (cm)		< 15	20 – 30		50 – 70		> 150	
Days with snow cover		< 30	60 – 80		100 – 120		> 160	
Climate classification		Cfb	Cfb		Dfb		Dfc	
Land cover		Agricultural land (*Sinapis alba*)	Meadow (*Agrostis capillaris, Festuca rubra*)		Forest (*Picea abies L.*)		Forest (*Fagus sylvatica L.*)	
Soil type		Regosol	Gleyc Fluvisol		Cambisol		Podzol	
Soil texture		Loamy sand	Sandy loam		Loamy sand		Loamy sand	
Retention curve parameters	Depth	20	20	40	20	40	20	40
	θ_r	0.05	0	0	0.18	0.18	0.10	0.06
	θ_s	0.39	0.50	0.50	0.51	0.52	0.65	0.45
	α	0.05	0.08	0.06	0.05	0.05	0.34	0.50
	n	1.74	1.20	1.18	1.37	1.70	1.45	1.34
	m	0.42	0.17	0.15	0.27	0.41	0.31	0.26
Reference		Seyedsadr et al. (2022)	Šípek et al. (2019)		Zelíková et al. (2025)		Vlček et al. (2021)	

Throughout the year, groundwater levels at most sites remain at least four meters below the soil surface. The ~~only exception is the~~ TD site represents the only exception, for wich~~, where~~ groundwater rises to approximately one meter below the surface during the spring months, potentially influencing the isotopic composition of the overlying soil profile. However, due to the sandy texture of the soil, capillary rise is limited, and this influence is therefore assumed to be confined to the lower soil layer sampled.

Each site was equipped with a meteorological station (Fiedler, Czechia) with rainfall gauges (Meteoservis, Czechia), Palmex precipitation collectors (Palmex Ltd., Zagreb, Croatia), and a tensiometer-regulated vacuum lysimeter system (VS-Pro, UMS, Germany) for ~~mobile soil water~~ MW sampling. Precipitation amounts, soil moisture, and air temperature were measured in 10-minute ~~steps~~ intervals and calculated on daily basis.

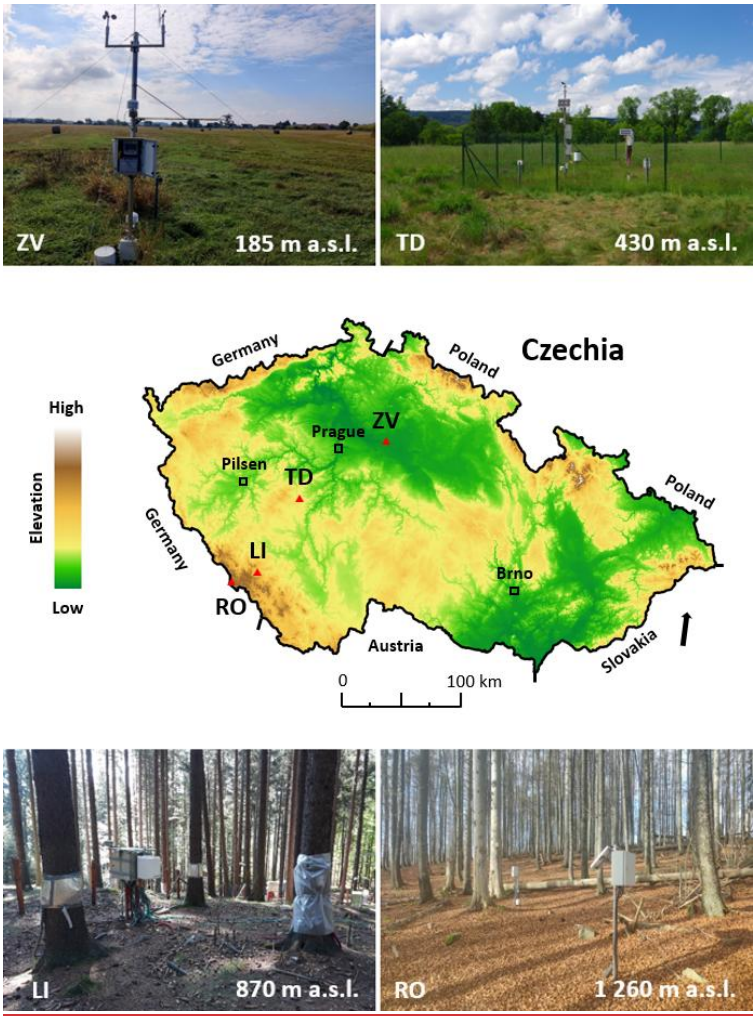
ZV
185 m a.s.l.
TD
430 m a.s.l.
Germany
Poland
Czechia
High
Elevation
Low
Prague
ZV
Pilsen
TD
Poland
Germany
LI
Brno
RO
Austria
Slovakia
0
100 km
LI
870 m a.s.l.
RO
1 260 m a.s.l.

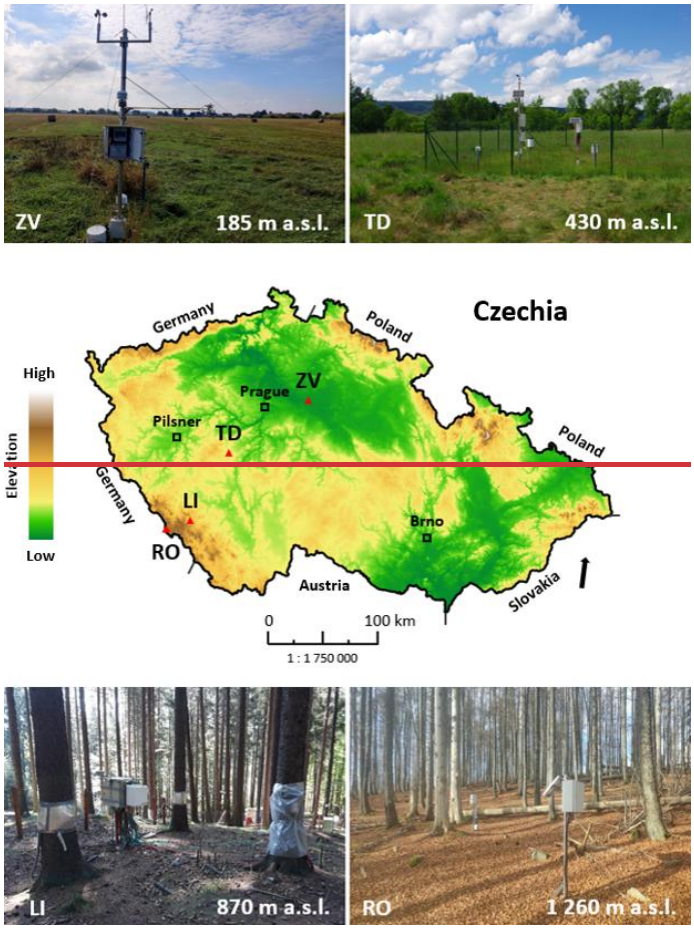

Figure 1. Location of selected experimental areas. Panels: top left – Zvěřínek; top right – Trhové Dušníky; bottom left – Liz; bottom right – Rokytka. Map data: Digital Vector Database of the Czech Republic ArcČR® version 4.3 (ARCDATA PRAHA, s.r.o., 2024).

3 Data and methods

3.1 Field sampling

At all study sites, precipitation was sampled at two-week intervals, except at the LI site, where samples were collected up to three times per week. Snow cover was sampled when present; however, the lower-elevation sites experienced sparse or no snow cover. For the comparison between precipitation and soil water, only precipitation samples from the respective hydrological year were used, as older water is not expected to persist at such shallow depths.

Furthermore, ~~samples of precipitation, mobile water (~~MW samples~~),~~ and soil cores for TBW extraction were collected at two-week intervals for the stable isotope analysis from February to November 2023. The exception was the RO location,

~~which was only~~ accessible only from May 2023 onwards due to its remote location in the heart of the Bohemian Forest National Park, as well as heavy snow conditions during winter and early spring.

~~For the extraction of~~ MW was extracted using a~~, the~~ tensiometer-controlled vacuum system (VS-Pro) ~~was employed~~ with a maximum applied tension of -60 kPa (Brooks et al., 2010; Berry et al., 2017; Sprenger et al., 2018). E~~The e~~xtraction was conducted ~~from~~ at two ~~two~~ depths of~~, specifically~~ 20 ~~cm~~ and 40 cm (hereafter referred to as D20 and D40, respectively); at the TD site, an additional depth of 60 cm was included~~,~~. These depths ~~which~~ often play a significant role in root water uptake (Hackmann et al., 2025). ~~Throughout the manuscript, these depths are referred to as shallow and deep layers, respectively.~~ Samples collected in this manner~~In both cases, the extracted samples~~ represent~~sed~~ a composite of water collected over the preceding two weeks.

For ~~the~~ TBW extraction, undisturbed soil cores (100 cm³) were collected from the same ~~two~~ depths, with five replicates per depth. The soil cores~~cylinders~~ were wrapped in Parafilm® and stored in a portable refrigerator during~~for~~ transport to the laboratory. In~~A~~ total, ~~of~~ 805 soil cores, 320~~9~~ MW samples, and ~~108~~ 195 precipitation samples were collected during the sampling period (Tab. 2).

Table 2. Overview of samples collected ~~at individual locations~~throughout the sampling period

		Number of samples / number of locations used for sampling			
Sample	Type	ZV	TD	LI	RO
Soil cores	D20	110 / 22	115 / 23	115 / 23	70 / 14
	D40	110 / 22	115 / 23	100 / 20	70 / 14
Mobile water	D20	74 / 6	42 / 3	31 / 2	8 / 1
	D40	23 / 3	50 / 3	26 / 2	8 / 1
	D60	-	58 / 3	-	-
Precipitation	Liquid	23	37	100	17
	Solid	1	2	11	4
Groundwater		-	9 / 1	-	-

The Type column indicates sampling depth (cm). For soil cores, the number of locations corresponds to the number of sampling campaigns (five samples per depth from a single soil profile per campaign). For mobile water, it represents the number of suction cups installed at the respective depths. For groundwater, it indicates the number of wells sampled.

3.2 Laboratory processing of soil samples

To obtain TBW, intact~~the~~ soil cores were placed~~inserted~~ in~~to~~ a~~the~~ pressure plate apparatus for the determination of the soil water retention curve ~~determination~~ (5 Bar Pressure Plate Extractor, Soil Moisture Equipment Corp., CA, USA), following a modified protocol based on Orlowski et al. (2020). ~~with a 1 bar pressure plate cell was used.~~ A pressure of 60 kPa (~ pF 2.4) was applied using a 1 bar pressure plate cell for a two-week period ~~was chosen to get rid of the~~to remove the MW fraction. Consequently~~Then~~, the top and bottom sections of each~~the soil~~ core were excised to eliminate portions potentially affected by contact with the ceramic plate and by evaporative losses.~~removed,~~ Only the central section of the core was retained for further extraction, yielding approximately 50 g of soil material per sample. ~~and for further extraction, only the inner soil core was used (approx. 50 g of soil sample).~~

For the subsequent extraction of TBW, the mass-balance mixing method was ~~selected~~ chosen due to its accessibility, simplicity and high throughput ~~(Fig. 2)~~. A comprehensive description of the method and validation through spike experiments for the investigated soil type is presented in the Supplementary Materials. Briefly, the experiments were carried out in the following steps:

- T~~t~~he soil samples (20–30g) were~~as~~ transferred~~placed~~ into 40 mL ~~a~~ glass vials (ND24 (EPA), ~~volume of 60 mL~~VERKON s. r. o., Czech Republic) equipped with~~with a~~ plastic screw caps fitted with~~and~~ silicone/PTFE septa~~aling~~ (VERKON s. r. o., Czech Republic).
- ~~Roughly~~ 20–25 mL of ~~a~~ isotopically labelled ~~traced~~ water (distilled tap water) was added to each~~the~~ sample, and the remaining headspace was filled with ~~glass balls (5 mm in diameter~~ glass beads (5 mm in diameter)~~)~~ to eliminate residual air and to enhance mechanical disaggregation of soil aggregates, thereby promoting efficient mixing (Fig. 2)~~to remove the presence of air~~.
- ~~-~~The vials~~n,~~ ~~the samples~~ were mounted~~placed~~ on a laboratory-constructed rotating device (Fig. S2) and continuously rotated~~spun~~ for 16 h~~ours~~ at a constant~~fixed~~ speed of 15 rpm.
- ~~. Subsequently, t~~The~~y~~ samples were ~~stored in a~~ refrigerated and left to settle~~or~~ to ~~to~~ allow sedimentation.~~mentation,~~
- ~~-~~A~~after which~~ 0.75 mL sample of the clear liquid phase~~mixture~~ was collected and filtered through a 0.45 µm mixed cellulose ester syringe filter ~~membrane~~. The remaining~~st~~ ~~of the~~ sample was oven-dried at 105 °C for 48 h~~ours~~ and weighed to determine~~calculate~~ the soil water content of the soil sample.

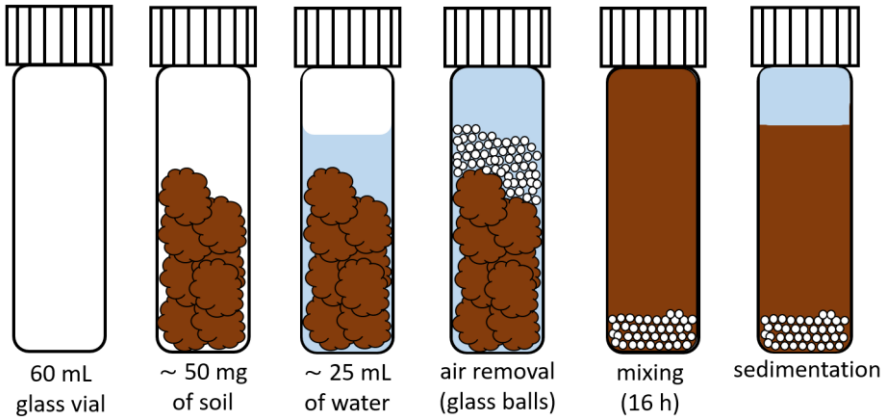

Figure 2. Sample processing procedure during the mass-balance mixing ~~extraction~~ method.

~~Prior to using this procedure, conventional spike experiments with labelled water were conducted to verify the accuracy of the extraction methods. This allows us to assess the method's performance for specific soil types collected from our study sites. The resulting isotopic shift relative to labelled water then incorporated into data correction procedures by subtracting this error from the final isotopic values, and the associated standard deviations were incorporated into the reported measurement uncertainties (together with the standard deviation of the real data and the measurement uncertainty of the isotope analyser).~~

3.3 Isotope analysis and calculations

Stable isotope analyses were performed at the Institute of Hydrology~~dynamics~~ (Czech Academy of Sciences) with a~~the~~ L2140-*i* isotope analyser (Picarro Inc., Santa Clara, US). Standard mode (precision of ± 0.03 ‰ and ± 0.15 ‰ for $\delta^{18}O$ and $\delta^{2}H$, respectively) was used with 6 injections per sample, out of them ~~with~~ the first 3 injections were discarded. The isotope ratios are reported in per mil (‰) relative to Vienna Standard Mean Ocean Water (VSMOW) ($\delta^{2}H$ or $\delta^{18}O = (R_{sample}/R_{standard}-1) \times 1000$ ‰, where R_{sample} is the isotope ratio of the sample and $R_{standard}$ is the known reference value (i.e., VSMOW), see ~~(~~Craig, (1961)~~)~~.

The isotopic composition of TBW was ~~then~~ calculated according to the mass balance mixing model (Eq. 1, 2).

$$\delta^{18}O_{STBW} = \frac{m_M}{m_{STBW}} \cdot \delta^{18}O_M - \frac{m_{TL}}{m_{STBW}} \cdot \delta^{18}O_{TL} \quad (1)$$

$$\delta^{2}H_{STBW} = \frac{m_M}{m_{STBW}} \cdot \delta^{2}H_M - \frac{m_{TL}}{m_{STBW}} \cdot \delta^{2}H_{TL} \quad (2)$$

where the sub-indices *M, TBW* and *L* denote the ~~represent~~ mixture ~~(*M*)~~, ~~TBW~~ tightly bound soil water~~(*S*)~~, and ~~traced~~ isotopically labelled water ~~(*T*)~~, respectively; *m* represents ~~is~~ the mass ~~weight~~ of water in each pool (determined gravimetrically using a pressure plate apparatus), with the total mass of the mixture given by $m_M = m_{TBW} + m_L$. ~~those waters and~~The terms $\delta^{18}O$ and $\delta^{2}H$ denote~~represent~~ the stable isotopic composition of the respective water pools~~sample~~.

Following the estimation of TBW, the ~~same~~ equivalent mass-balance mixing model was applied to calculate the potential stable isotopic composition of BW. In this approach, BW was represented as a mixture of MW, obtained from suction lysimeters, and TBW, as derived in the previous step. The relative proportions of these two components were determined based on measurements from the pressure plate apparatus.

To establish the local meteoric water lines (LMWLs) and regression lines for soil water isotopic compositions, a reduced major axis (RMA) regression was applied (Harper, 2016) instead of the conventional linear regression. A necessity of the application of the RMA regression is caused by significant uncertainties in both δ^2H and $\delta^{18}O$ measurements, moreover in the case of soil water, substantially increased by the mixing-extraction method, systematically introducing a shift. In contrast, isotopic measurements of precipitation were associated primarily with analytical precision only. Since the classical least squares regression a priori assumes that all errors are related to the y-axis only and entirely ignores uncertainties along the x-axis, the RMA regression was considered appropriate for both soil water and precipitation, providing a more accurate representation of the δ^2H–$\delta^{18}O$ relationship by minimizing the orthogonal distances between data points and the fitted approximation.

The slope β_{RMA} (Eq. 3) of the RMA regression was calculated as the ratio of the standard deviations of δ^2H and $\delta^{18}O$, multiply by the sign of their Pearson correlation coefficient, and the intercept αRMA (Eq. 4) was determined as the difference between the mean δ^2H and the product of the slope and mean $\delta^{18}O$:

$$\beta_{RMA} = sign(r) \cdot \frac{\sigma_{\delta^2 H}}{\sigma_{\delta^{18} O}} \quad (3)$$

$$\alpha_{RMA} = \overline{\delta^2 H} - \beta_{RMA} \cdot \overline{\delta^{18} O} \quad (4)$$

where r is the Pearson correlation coefficient between δ^2H and $\delta^{18}O$, and $\sigma_{\delta^2 H}$ and, $\sigma_{\delta^{18} O}$ are their standard deviations. This method minimizes the orthogonal distances between data points and the fitted line, making it suitable for hydrological isotope data where both variables are subject to analytical and natural variability.

To quantify the uncertainty of the RMA regression predictions, a bootstrap procedure with 10,000 resamples was applied. For each bootstrap iteration, a dataset of equal size was sampled with replacement, the RMA regression coefficients were recalculated, and residual variation was added to generate a distribution of predicted δ-values. 95 % confidence intervals were derived at each $\delta^{18}O$ value from the 2.5th and 97.5th percentiles of these predicted values, providing prediction intervals for the regression lines.

The slopes of the regression lines were compared among different data sets (precipitation, MW, TBW) using their bootstrap distributions. For each comparison, differences between bootstrap slopes were calculated, and 95 % confidence intervals of these differences were obtained. A slope difference was considered statistically significant if the 95 % interval did not include zero. Additionally, pseudo-R^2 values were calculated as the squared Pearson correlation coefficient for each dataset within the aim to indicate the goodness-of-fit.

Furthermore, the line-condition excess (*lc-excess*; Landwehr and Coplen, 2006) was ~~calculated~~ determined (Eq. ~~3~~5) to identify and exclude data contaminated during the water extraction process.

$$lc - -excess = \delta^2H - a \cdot \delta^{18}O - b \quad (~~3~~5)$$

where *a* and *b* are the coefficients of the ~~local meteoric water line (~~LMWL~~)~~ from the individual experimental plots. This contamination was manifested by abnormally high *lc-excess* values relative to the rest of the dataset. An *lc-excess* value of 10 was taken as a pragmatic screening threshold; however, this criterion was not applied rigidly. Values slightly exceeding 10 were retained in the final dataset when the overall distribution of the respective sample group remained below or close to this threshold. In contrast, apparently contaminated samples, typically exhibiting *lc-excess* values between 20 and 50, were removed entirely. In such cases, all associated measurements were excluded, as well as occasional values marginally below 10, when they represented isolated initial observations followed by consistently elevated *lc-excess* values within the same sample set.

The methodological nature of the error was further supported by the observation that these anomalous values appeared randomly across different sites and sampling dates, with the only consistent factor being that the affected samples were processed together within the same run of the overpressure apparatus. In total, 6 out of 32 extraction runs of TBW_~~,~~ ~~corresponding to approximately 98 out of 805 soil samples, had to be~~were discarded due to this methodological error and significant sample contamination.

~~For the seasonal comparison of the stable isotopic composition of mobile and tightly bound soil water, seasons were defined as follows: winter (F), spring (MAM), summer (JJA), and autumn (SON).~~

~~3.4 Data fitting~~

~~To visualize the stable isotope data and characterize their seasonal variability, a sine function was fitted to the data using the iteratively reweighted least squares (IRLS) regression method with externally supplied weights in case of precipitation data (Eq. 4), a technique commonly applied to characterize the seasonal cycle of precipitation, streamflow, soil water, and groundwater (Kirchner, 2016; Zuecco et al., 2024; Floriancic et al., 2024; Xia et al., 2024). From the Eq. 4, the amplitude can then be determined according to the Eq. 5:~~

$$~~c(t) = a \cdot cos(2\pi ft) + b \cdot \sin(2\pi ft) + k~~ \quad (~~4~~)$$

$$~~A = \sqrt{a^2 + b^2}~~ \quad (~~5~~)$$

~~where *t* is the time, *c(t)* represents the isotopic time series of the dataset, *a* and *b* are the cosine and sine coefficients determined by the IRLS regression, *f* is the frequency of annual isotopic fluctuation (*f* = 1 yr^{-1} for a seasonal cycle), *k* is the vertical shift of the sine wave, and *A* is the amplitude of the fitted sine wave.~~

~~Since the soil water and groundwater often lack a consistent seasonal signal, it is hard to fit them with a fixed sine wave, especially when spanning multiple seasons (Xia et al., 2024). Therefore, in some cases a weighted third-degree polynomial fit was used to provide a clear visualization of the stable isotopic composition throughout the year.~~

~~To establish the LMWLs and regression lines for soil water isotopic compositions, reduced major axis (RMA) regression was applied (Harper, 2016) instead of conventional linear regression. This approach was selected because uncertainties in both δ^2H and $\delta^{18}O$ measurements are equally significant, whereas ordinary least squares regression assumes all error is confined to the y-axis and ignores uncertainty in the x-axis.~~

~~The slope (Eq. 6) of the RMA regression was calculated as the ratio of the standard deviations of δ^2H and $\delta^{18}O$, scaled by the sign of their Pearson correlation coefficient. The intercept was then calculated according to Eq. 7:~~

$$\beta_{RMA} = sign(r) \cdot \frac{\sigma_{\delta^2 H}}{\sigma_{\delta^{18} O}} \quad (6)$$

$$\alpha_{RMA} = \overline{\delta^2 H} - \beta_{RMA} \cdot \overline{\delta^{18} O} \quad (7)$$

~~where α_{RMA} and β_{RMA} are the intercept and slope of the RMA, respectively, r is Pearson correlation coefficient between δ^2H and $\delta^{18}O$, and $\sigma_{\delta 2H}$, $\sigma_{\delta 18O}$ are their standard deviations. This method minimizes the orthogonal distances between data points and the fitted line, making it more suitable for hydrological isotope data where both variables are subject to analytical and natural variability.~~

3.~~5~~ 4 Seasonal Origin Index (SOI)

To characterize whether the extracted soil water originated from winter or summer precipitation, ~~we calculated~~ the Seasonal Origin Index (SOI) was calculated (Eq. ~~8~~6; ~~)~~ (Allen et al., 2019) for individual ~~seasons, as well as for individual months~~sampling dates, to provide a more detailed representation of gradual changes in water origin resulting from mixing with newly infiltrating water.

$$SOI = \begin{cases} \dfrac{\delta_x - \delta_{annP}}{\delta_{summerP} - \delta_{annP}} & \text{~~if~~ for } \delta_x > \delta_{annP} \\ \dfrac{\delta_x - \delta_{annP}}{\delta_{annP} - \delta_{winterP}} & \text{~~if~~ for } \delta_x < \delta_{annP} \end{cases} \quad (8)$$

where δ_x denotes~~are~~ the $\delta^{18}O$ isotopic composition ~~values~~ of soil water, and δ_{annP}, $\delta_{winterP}$, and $\delta_{summerP}$~~,~~ represent~~are~~ the $\delta^{18}O$ ~~isotopic~~ values of volume-weighted annual precipitation, the characteristic ~~typical~~ winter (δ_{annP} – fitted amplitude)~~,~~ and ~~typical~~ summer (δ_{annP} + fitted amplitude) precipitation, respectively. These precipitation components were derived from sinusoidal fitting to the time series. Prior to analysis, samples with negative *lc-excess* were corrected according to Benettin et al. (2019) to account for potential biases in isotope measurements.

Specifically, a sine function was fitted to the isotope data using an iteratively reweighted least squares (IRLS) regression approach with externally supplied weights for precipitation (following the methodology of Kirchner, 2016). This approach is widely applied to quantify the seasonal isotope cycle in precipitation, streamflow, soil water, and groundwater. The fitted amplitude was subsequently obtained from Eq. (7) and calculated according to Eq. (8). ~~The SOI ranges from −1 to 1, where values close to −1 represent water predominantly derived from winter precipitation, and values approaching 1 reflecting a dominant contribution from summer precipitation.~~

$$c(t) = a \cdot cos(2\pi ft) + b \cdot \sin(2\pi ft) + k \quad (7)$$

$$A = \sqrt{a^2 + b^2} \quad (8)$$

~~**3.6 Statistical evaluation**~~

~~To statistically assess the differences in annual courses of isotopic composition of individual waters (MW, TBW), it was necessary to consider the uncertainty in the coefficients of the regression models. Therefore, following the approach of Davison and Hinkley (1997), bootstrap residual resampling was performed as follows:~~

~~1. Regression models f_A and f_B were fitted to datasets A and B (Y; e.g., MW and TBW), and residuals (r_A, r_B) were calculated (Eq. 9, 10).~~

$$r_{A,t} = f_{A,t} - Y_{A,t} \quad (9)$$

$$r_{B,t} = f_{B,t} - Y_{A,t} \quad (10)$$

~~2. The following steps were repeated 10,000 times:~~

~~a. Synthetic datasets were generated (Eq. 11, 12).~~

$$Y_{A,boot,t} = f_{A,t} + r_{A,rand} \quad (11)$$

$$Y_{B,boot,t} = f_{B,t} + r_{B,rand} \quad (12)$$

~~where r_A,rand and r_B,rand are randomly sampled residuals (with replacement).~~

~~b. New regression curves f_A,boot and f_B,boot were fitted to the synthetic datasets.~~

~~c. The difference between the curves was computed and stored (Eq. 13).~~

$$d = \int |f_{A,boot} - f_{B,boot}| \quad (13)$$

**where t is the time, $c(t)$ represents the isotopic time series of the dataset, a and b are the cosine and sine coefficients determined by the IRLS regression, f is the frequency of annual isotopic fluctuation (f = 1 yr^{-1} for a seasonal cycle), k is the vertical shift of the sine wave, and A is the amplitude of the fitted sine wave.~~~~A 95% confidence interval for the curve difference was derived as a range between the 0.025 and 0.975 quantiles of the resampled differences.~~

~~3. The samples were considered significantly different if the confidence interval did not contain zero.~~

4 Results

4.1 Precipitation and soil water data

The collected data closely follow the LMWLs of the respective locations, however, a clear difference is observed for TBW, which follows the LMWL with greater dispersion. In comparison with MW, several samples lie outside the 95% prediction

interval for precipitation (Fig. 3), indicating the influence of isotopic fractionation associated with evaporation and subsequent condensation and internal mixing processes within the soil matrix.

~~Given~~ Due to the pronounced elevation gradient between ~~geographical proximity of~~ the study sites, a systematic shift in both the slope and intercepts of the LMWLs was~~ere~~ observed~~similar across all locations (Fig. 3)~~. The ZV lowland agricultural site (on average 150 m a.s.l.) is characterized by a reduced slope~~, ranging from~~ (7.6) and a low intercept~~7 to 8~~ (3.7), indicative of enhanced sub-cloud evaporation and stronger kinetic fractionation under warmer and drier boundary-layer conditions (Tab. 3). ~~In contrast, the y-intercepts varied considerably, from 4.2 to 11.5.~~ Both parameters increase with~~reflected the~~ elevation ~~gradient~~, reaching ~~with the lowest~~ values of 8.2 (slope) and 13.6 (intercept) ~~recorded~~ at the ~~lowland ZV site and the~~ highest-elevation site, ~~at the mountainous location~~ RO (on average 1100 m a.s.l.). These values suggest limited secondary evaporation and a greater contribution of equilibrium-controlled condensation associated with orographic uplift. ~~narrower isotopic range observed at the RO site was likely due to the incomplete dataset, as sampling was limited to the period between May and November~~These observed differences are therefore primarily attributed to the elevation-dependant climatic conditions.

Mobile soil water (MW) closely tracked the LMWLs, with slopes ranging from 7.4 to 8.2~~1~~ and intercepts from 2.0 to ~~1~~15.8, suggesting minimal isotopic fractionation associated with ~~alteration by~~ evaporation or subsequent condensation processes. However, its isotopic range was narrower and ~~often~~ on average more depleted than that of precipitation. ~~This depletion likely resulted from the absence of winter precipitation data (December and January), which typically exhibits more negative isotopic values.~~ Similar to precipitation, an elevation trend was also apparent in the isotopic composition of MW.

In contrast, ~~no consistent elevation pattern was observed for~~ TBW exhibited a reversed elevation trend both in slope (6.6–7.8) and in intercept (0.3–6.5) values decreasing with elevation. The differences became most pronounced at higher elevations. The differences between slopes were assessed using bootstrap resampling applied to the RMA regressions. At the high-elevation sites, most slope differences were significant, whereas the slopes of precipitation and MW at RO, and those of MW and TBW at LI, were not significantly different at the 95% confidence level. In contrast, at lowland sites, no significant differences among the slopes of the regression lines were observed. ~~Unlike MW and precipitation, TBW exhibited clear signs of evaporative enrichment and isotopic modification due to condensation and internal mixing processes within the soil matrix. These effects were reflected in lower slopes (ranging from 5.9 to 7.5) and a broader dispersion of data around the respective soil water evaporation lines.~~

Table 3. RMA regression parameters (slope and intercept) along with their corresponding standard deviations (SD), estimated using bootstrap analysis.

Study site	Dataset	Slope ± SD	Intercept ± SD
ZV	Precipitation	7.6 ± 0.2	3.7 ± 1.4
	MW	7.4 ± 0.1	2.0 ± 0.7

	TBW	7.8 ± 0.2	6.5 ± 2.0
TD	Precipitation	7.6 ± 0.2	5.8 ± 2.0
	MW	7.7 ± 0.2	6.7 ± 1.8
	TBW	7.4 ± 0.5	5.3 ± 4.7
LI	Precipitation	8.0 ± 0.1	8.6 ± 0.8
	MW	7.6 ± 0.1	5.6 ± 1.3
	TBW	7.1 ± 0.4	0.7 ± 3.7
RO	Precipitation	8.2 ± 0.2	13.6 ± 1.6
	MW	8.2 ± 0.3	15.8 ± 3.1
	TBW	6.6 ± 0.4	0.3 ± 4.0

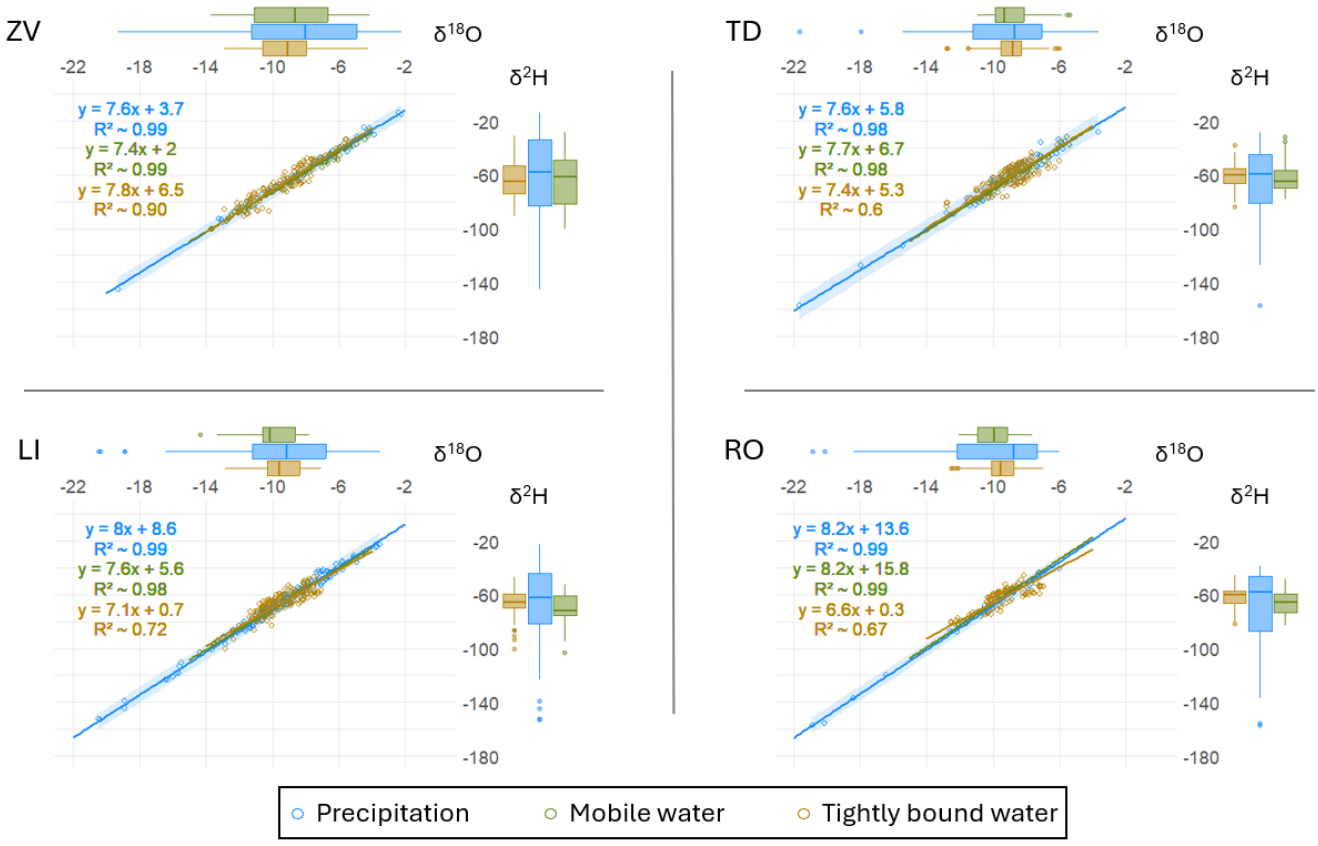

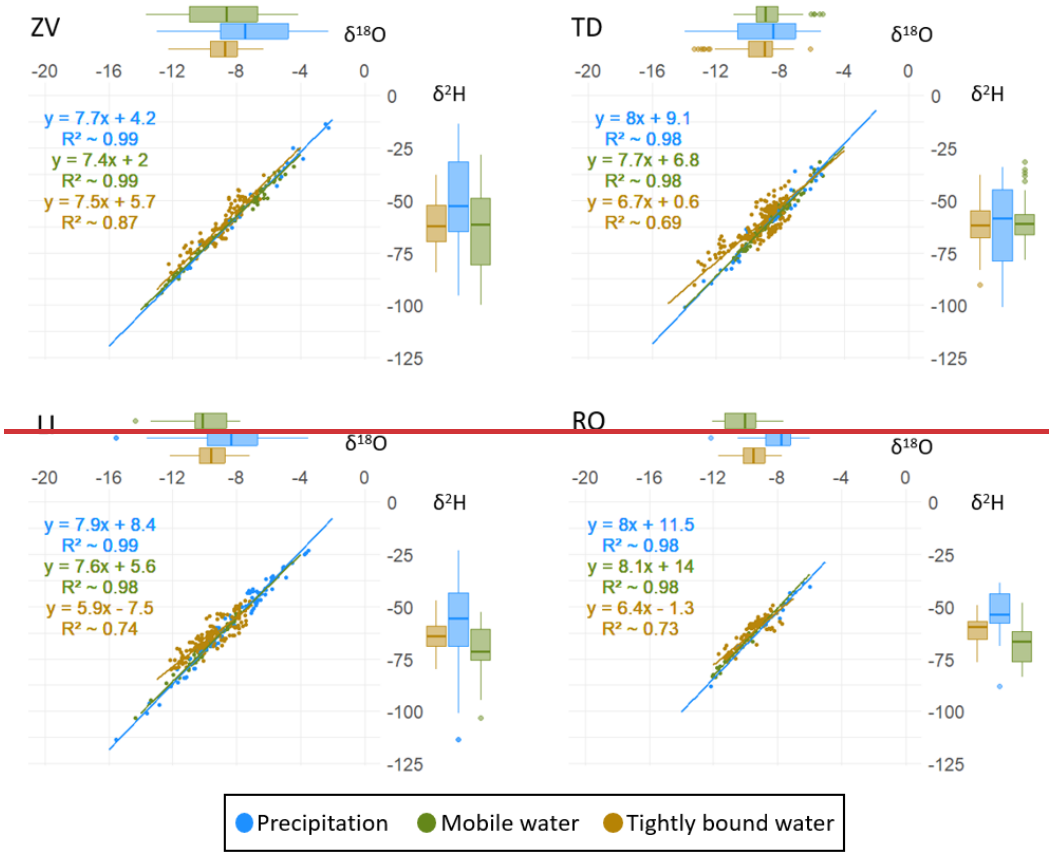

Figure 3. Dual-isotope plots of all water samples collected in this study, with corresponding regression lines. Panels: top left – ZV (lowland agricultural field)~~Zvěřínek~~; top right – TD (mid-elevation meadow)~~Trhové Dušníky~~; bottom left – LI (submontane spruce forest)~~Liz~~; bottom right – RO (montane beech forest)~~Rokytka~~. Precipitation is shown in blue, mobile soil water in green, and tightly bound soil water in brown. Blue shading shows the 95% prediction interval for precipitation.

4.2 Comparison of mobile and tightly bound soil water

The d~~A d~~ifferences in stable isotopic composition between~~of~~ MW and TBW were~~as~~ observed at all~~cross~~ experimental sites (~~Fig. 4~~). Among all components, D20~~shallow~~ MW exhibited the greatest annual isotopic variability. At the ZV site, this variability reached 7.6 ‰ and 57.2 ‰ for $\delta^{18}O$ and $\delta^{2}H$, respectively, but decreased with increasing elevation to only 5.6 ‰ and 43.2 ‰ at the LI site (Fig. 4). The largest contrast between D20 MW and TBW occurred in spring and autumn, with the maximum difference recorded on 7 March 2023 at the ZV site (3.3 ‰ and 20.7 ‰ for $\delta^{18}O$ and $\delta^{2}H$, respectively).~~However, this variability diminished with increasing elevation. In lowland areas, deep soil water tended to be more isotopically depleted compared to shallow layers, but this trend weakened or even reversed at higher elevations.~~

~~The most pronounced contrasts between MW and TBW were recorded in spring and autumn, and to a lesser extent during summer at the TD site. At the ZV site, isotopic differences between shallow and deep soil water, both MW and TBW, became evident primarily in the second half of the year when shallow soil water was being replaced by the summer precipitation. In contrast, at the mountainous sites (LI, RO), the largest differences between shallow and deep MW occurred in the first half of the year, while the isotopic composition of TBW remained relatively stable throughout the study period.~~ A distinct phase shift between D20 MW and TBW was observed between February and May at all sites except RO (Fig. S1). The largest lag occurred at the ZV site, where the response of soil water to precipitation exceeded three months, representing the slowest response across the gradient. The lag decreased with elevation, shortening to approximately six weeks at LI site and becoming negligible at the highest-elevation site. The rapid response at the highest site likely reflects high annual precipitation (~1,400 mm), which frequently flushed the saturated soil profile. D40 MW and TBW exhibited broadly similar temporal dynamics and phase relationships to those observed for D20 TBW across all sites.

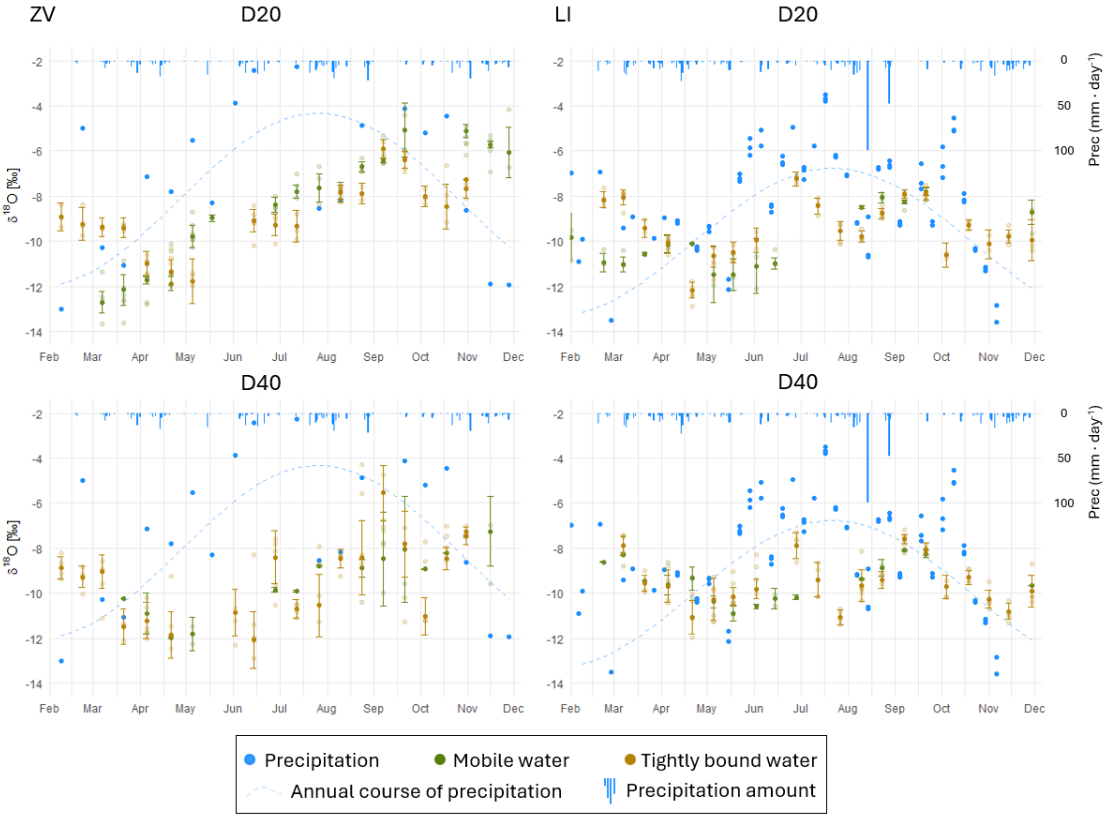

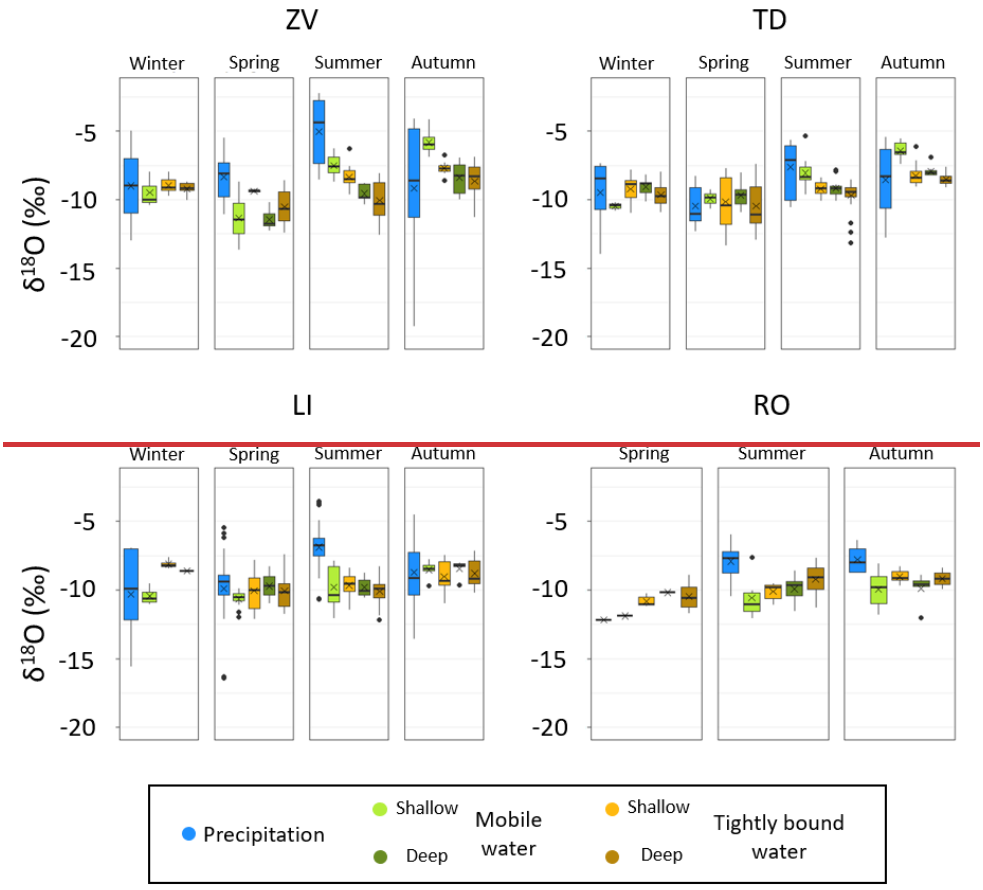

Figure 4. Seasonal comparison of the stable isotopic compositions of mobile and tightly bound soil water at two depths ~~-~~at selected~~the~~ study sites (the remaining two sites are shown in the Supplement, Fig. S1). Left p~~P~~anels: ~~top left —~~ZV (lowland agricultural field)~~Zvěřínek~~; ~~top~~ right panels:~~—~~ LI (submontane spruce forest)~~Trhové Dušníky~~. Blue rectangles denote the daily precipitation (mm), and the light-blue dashed sine curve represents the weighted fit of the annual cycle of precipitation isotopic composition.~~; bottom left — Liz; bottom right — Rokytka. Seasons are defined as follows: winter (F), spring (MAM), summer (JJA), and autumn (SON). Boxplots are presented in the same order across panels, except for winter at the Liz site, where deep tightly bound soil water data are missing.~~

~~In most cases, the isotopic composition of soil water closely reflected that of precipitation during the corresponding time period. A notable exception was observed at the ZV site, where the response time of soil water to precipitation exceeded three months, making it the slowest among all sites. Another distinct anomaly was detected at the LI site during the summer, where soil water showed no clear isotopic response to recent rainfall. This lack of response is attributed to an intense precipitation event (>100 mm in two hours), which had an isotopic composition of approximately −10‰ for $\delta^{18}O$, and effectively stabilized the isotopic signature of soil water around this value.~~With the onset of the dry season and severe drought

in July, soil profiles nearly dried out and isotopic differences among soil water pools diminished. With the decline of autumn period, isotopic amplitude peaks became synchronized, resembling the pattern of D20 MW but with attenuated signals. This attenuation likely resulted from mixing between newly infiltrated precipitation and residual water stored in the profile. Despite this homogenization, a temporal offset between precipitation and MW persisted at all sites except RO.

The influence of precipitation on soil water isotopic composition increased with elevation and precipitation input. At lower elevations (e.g., ZV) new precipitation gradually diluted pre-existing soil water, resulting in progressive isotopic enrichment. In contrast, at higher elevations, large precipitation inputs often replaced older soil water, resulting in soil water isotopic composition close to that of precipitation. Consequently, soil water in both horizons—particularly at the RO site (Fig. S1)—showed high variability and limited predictability.

~~4.3 Influence of the elevation gradient on the lag in soil water pool dynamics~~

~~Significant differences between MW and TBW were observed across the elevation gradient, both in their absolute quantities and their stable isotopic composition. With increasing elevation and precipitation amounts, the volumetric soil water content increased across the study sites (Fig. 5). At the lowest elevation sites (ZV, TD), the average water content was approximately 23 g per 100 cm^3 of soil at both, 20 cm and 40 cm depths, with slightly higher values in 20 cm, whereas at the highest site (RO) it reached up to 47 g per 100 cm^3 at both depths, again with slightly higher values in the upper layer. Furthermore, the influence of snow cover, increased precipitation, and lower temperatures (resulting in a delayed onset of the growing season and generally reduced evapotranspiration) was reflected in a gradual increase in soil water content during spring and early summer at higher elevation sites. In contrast, in lowland areas, soil water content tended to plateau after the winter season due to full saturation of the soil profile. Following the onset of the growing season, accompanied by increased evapotranspiration and progressive soil drying, the soil water content began to decline at all sites.~~

~~In terms of stable isotopic composition, significant phase shifts between precipitation and various soil water pools were observed both among the study sites and within individual locations over the course of the year. The most pronounced lag between precipitation and shallow MW occurred at the ZV site, where the temporal offset exceeded three months (Fig. 5). This lag decreased along the elevation gradient by shortening to approximately six weeks at the mid-altitude site and becoming negligible at the highest elevation site.~~

~~Furthermore, at all locations except the RO site, a distinct phase shift between shallow MW and TBW was observed between February and May, with the magnitude of this shift decreasing with increasing elevation. Deep soil water compartments generally exhibited similar temporal dynamics and phase lags as shallow tightly bound water, although they tended to be more isotopically depleted, hence contained more water from winter precipitation. An exception was found at the TD site, where the isotopic compositions of deep MW and TBW were different. Moreover, we hypothesize that the seasonal pattern of shallow TBW at the RO site would resemble that of the deep soil water pools. However, due to the limited number of data points available, all fitting approaches applied (both weighted and unweighted sine functions, as well as polynomial models) yielded comparable results, as illustrated in Fig. 5.~~

Following the onset of the dry season, the isotopic differences among soil water pools gradually diminished. By the end of the year, amplitude peaks became synchronized, resembling the pattern of shallow MW, though with attenuated isotopic signals. This attenuation likely resulted from mixing between newly infiltrated precipitation and residual water from previous periods. Despite this homogenization, a temporal offset between precipitation and MW remained evident. The negligible lag observed at the highest site was likely due to the high annual precipitation (~ 1,400 mm), which rapidly flushed the saturated soil profile.

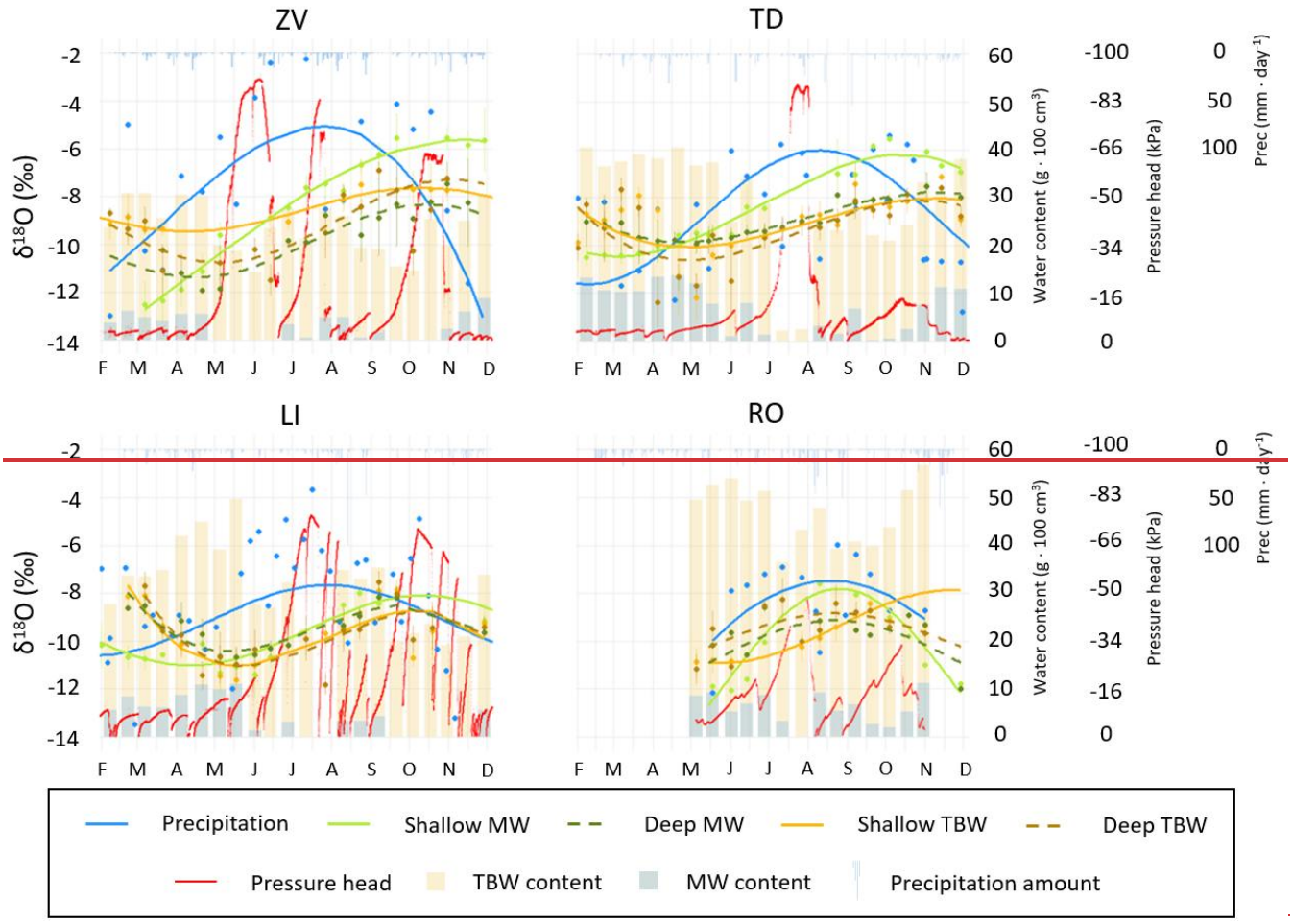

Figure 5. Annual variation in the isotopic composition of soil water in relation to soil water content, pressure head, and precipitation amounts. Both soil water content and pressure head refer to a depth of 20 cm. Panels: top left – Zvěřínek; top right – Trhové Dušníky; bottom left – Liz; bottom right – Rokytka.

The influence of the elevation gradient was further supported by the bootstrap residual analysis, which revealed statistically significant differences in the seasonal dynamics of the stable isotopic composition of soil water pools. These differences were more pronounced in lowland areas (Table 3). Among the four pairwise comparisons assessed (shallow MW vs. TBW; deep MW vs. TBW; shallow vs. deep MW; and shallow vs. deep TBW), the most consistent differences were observed between shallow and deep MW. This contrast was statistically significant in three out of four cases, with the exception of the LI site, where – despite apparent differences early in the year – the statistical test did not confirm significance.

For the comparison between deep MW and TBW at the ZV and TD sites, no statistically significant differences were detected; however, the null hypothesis was rejected only marginally, with the critical zero threshold exceeded by just 0.07 and 0.03, respectively.

In the case of shallow MW vs. TBW at the ZV site, a statistical difference was not confirmed, despite clearly distinct isotopic signatures (Fig. 5). This outcome likely reflects a limitation of the applied statistical method, which lacks sensitivity to detect differences in symmetrically distributed data. A similar limitation may also affect the comparison between shallow and deep MW at the RO site. However, the two instances confirming the null hypothesis at this site were more likely due to a lack of the TBW data and their unrepresentative interpolation using a sine curve (Fig. 5).

Table 3. The results of the bootstrap residual resampling analysis. H_0: Fitted sine functions are statistically different. The H_0 is rejected if the interval between q025 and q975 contains zero.

Compared combinations	Quantiles	Locations			
		Zvěřínek	Trhové Dušníky	Liz	Rokytka
Shallow MW vs. Shallow TBW	q025	-0.44	-1.19	-0.20	1.42
	q975	0.40	-0.29	1.40	2.62
	Result	False	True	False	True
Deep MW vs. Deep TBW	q025	-0.07	-0.83	-0.69	-0.82
	q975	1.11	0,03	0.76	1.25
	Result	False	False	False	False
Shallow MW vs. Deep MW	q025	0.65	0.33	-1.27	-2.33
	q975	1.68	0.80	0.23	-0.67
	Result	True	True	False	True
Shallow TBW vs. Deep TBW	q025	0.12	-0.36	-0.69	-0.58
	q975	1.15	0.83	0.83	1.13
	Result	True	False	False	False

4.4 3 Origin of the soil water

Seasonal Origin Index (SOI; Fig. 5) values exhibited a consistent transition from winter-dominated signals in spring to summer-dominated signals later in the growing season across all sites. Site-specific differences reflected elevation-related

gradients in precipitation and hydrological dynamics: higher-elevation forest sites (LI, RO) showed a stronger dominance of summer precipitation, whereas lower-elevation sites (ZV, TD) retained a more mixed seasonal signal. Moreover, the seasonal increase in SOI became steeper in mountainous areas, indicating a more rapid shift from winter- to summer-dominated precipitation and a shorter transitional period between these seasonal regimes. For the RO site, earlier seasonal data are not available (as explained above); however, the relatively high SOI values observed soon after snowmelt, together with the highest precipitation totals among the study sites, suggest that the seasonal turnover may be even more pronounced than at the LI site. ~~The results of water origin analyses revealed distinct temporal patterns in the SOI across the study sites. Among the soil water components, shallow MW showed the highest isotopic variability, with the magnitude of fluctuations decreasing along the elevation gradient. Within the soil profile, the lowest SOI values, indicating a predominant contribution of winter precipitation, were typically recorded in spring, whereas the highest values, reflecting a dominant influence of summer precipitation, occurred in autumn (Fig. 6).~~

~~The influence of winter precipitation remained detectable in the soil profile until late summer at all sites except the highest elevation site, RO. This pattern was evident across all soil water compartments except shallow MW, which was already affected by summer precipitation during the summer months. At the RO site, the data obtained indicate that influence of winter precipitation had already diminished by May. Although this assessment may be influenced by the absence of data from previous months.~~

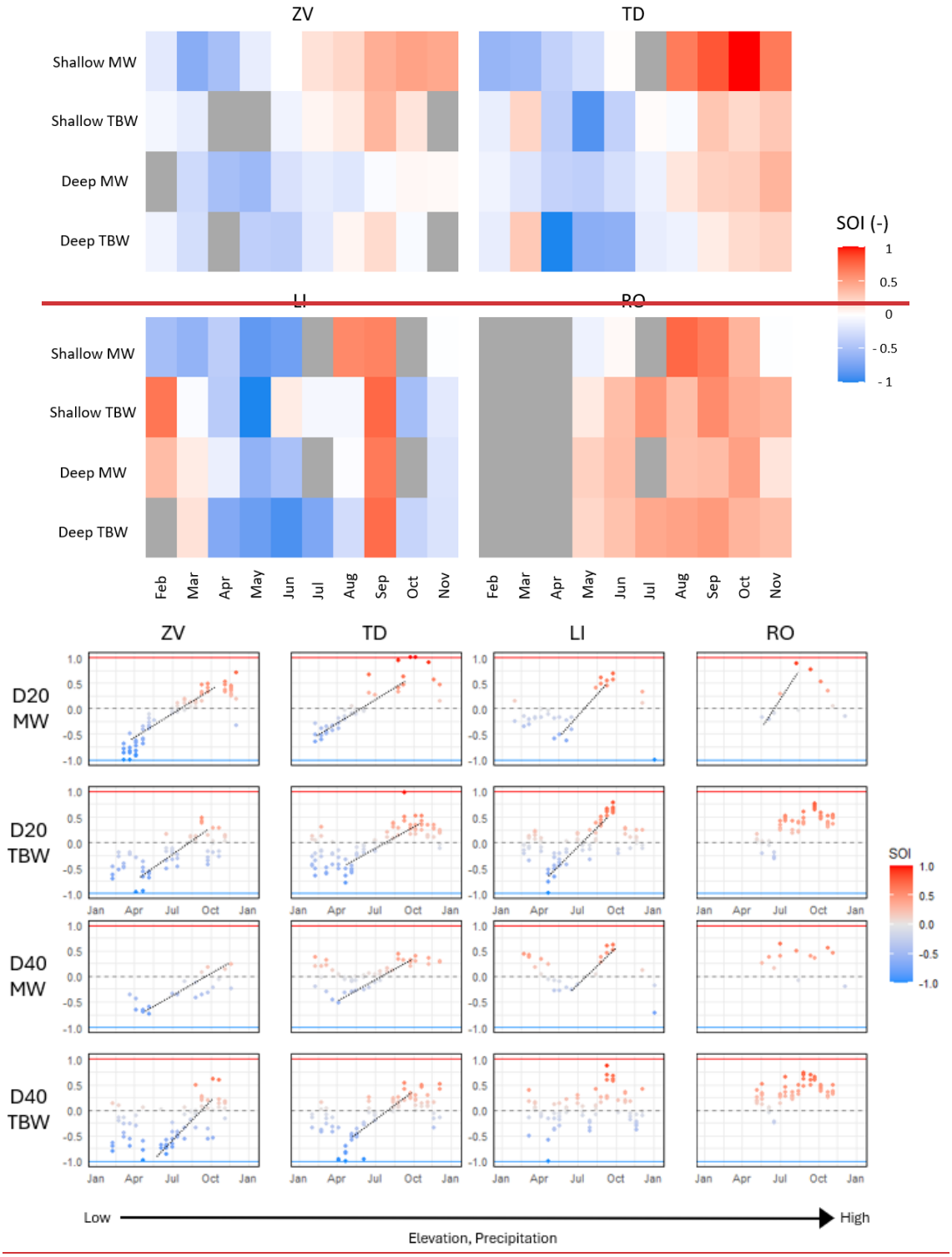
ZV
TD
LI
RO
Shallow MW
Shallow TBW
Deep MW
Deep TBW
SOI (-)
1
0.5
0
- 0.5
- 1
Feb
Mar
Apr
May
Jun
Jul
Aug
Sep
Oct
Nov
D20 MW
D20 TBW
D40 MW
D40 TBW
SOI
Jan
Apr
Jul
Oct
Low
High
Elevation, Precipitation

Figure ~~6~~5. Seasonal origin index (SOI) values ~~for individual~~across sites, depths, and soil water pools throughout the year 2023~~months~~. Panels represent four study sites: ZV (lowland agricultural field), TD (mid-elevation meadow), LI (submontane spruce forest), and RO (montane beech forest). Soil water was sampled at two depths (D20 = 20 cm; D40 = 40 cm). ~~The abbreviations~~ MW and TBW denote~~refer to~~ mobile water and tightly bound soil water, respectively. SOI ~~V~~values near −1 indicate a ~~pre~~dominant contribution from winter precipitation, whereas values approaching +1 reflect a dominant contribution from summer precipitation. Point colours represent SOI magnitude. The dashed black line illustrates the seasonal transition from winter- to summer-dominated precipitation inputs. ~~Grey areas indicate missing data for the respective period. Panels: top left – Zvěřínek; top right – Trhové Dušníky; bottom left – Liz; bottom right – Rokytka.~~

The differences between water pools were most evident at the lower-elevation sites (ZV and TD), where the transition from winter- to summer-dominated precipitation was delayed both between water pools at the same soil depth (e.g., July for MW vs. approximately August for TBW at D20 at the ZV site) and with increasing soil depth within the same water pool (August for D20 TBW vs. September for D40 TBW). Furthermore, D20 MW followed the annual course of precipitation most closely, whereas all other water pools exhibited a delayed response, particularly during the first half of the year, and retained an SOI signal from precipitation of the previous year. However, following a severe drought in July–August, the soil profiles were replenished by current precipitation. Consequently, the delay relative to precipitation was reduced, and differences among individual water pools largely disappeared, except for D20 MW.

~~The highly positive SOI values observed in autumn at the TD site were attributed to a period of severe drought in July, which desiccated the upper soil layers (Fig. 5), followed by rewetting from late-summer rainfall. SOI values increased steadily from August to October and subsequently declined, closely mirroring the isotopic composition of precipitation during this period. Conversely, the strongly negative SOI values recorded in spring were likely caused by a rising groundwater table. This would explain their earlier appearance in deeper soil layers and delayed onset in shallower horizons. Notably, despite the fact that the proportion of MW in the deeper soil layer reached up to 64% relative to TBW at the beginning of the year, there was no isotopic homogenization between these two water pools, and both components remained isotopically distinct. Furthermore, we attribute the alternation of negative and positive SOI values at the TD site early in the year to preferential flow, which may have influenced the February samples of tightly bound water. We further hypothesize that the isotopic composition during this period would resemble that at the LI site, where water from the previous summer and autumn was retained and delayed within the soil profile.~~

~~The markedly positive SOI values observed in September at the LIZ site were linked to the second most intense precipitation event of the year, nearly 50 mm, characterized by an isotopic composition of −6.55‰ for $\delta^{18}O$ and −43.36‰ for $\delta^{2}H$, which saturated the otherwise relatively dry soil profile.~~

4.~~5~~ 4 Bulk soil water

Although BW was not directly sampled in this study, we present a conceptual illustration of its potential isotopic composition based on the obtained data. The results showed, that the stable isotopic composition of BW, estimated indirectly using a mass-balance mixing model (Eqs. 1 and~~,~~ 2), may vary statistically from TBW for both $\delta^{18}O$ and $\delta^{2}H$. The u~~U~~npaired t-test ($P < 0.05$) revealed this difference on at least one sampling date at both lowland study site (ZV, TD), with no difference observed at higher elevations. During the summer drought period, however, when soil desiccation removed almost all MW from the soil profile, BW effectively represented solely TBW~~ alone~~.

Since the isotopic signature of BW depends both on~~ both,~~ the relative proportions of MW and TBW, and the isotopic contrast between them, the greatest deviations were observed during the spring and autumn seasons. During these periods, both the isotopic differences ~~between~~ among water pools and the proportion of MW in the soil reached their annual maxima ~~(Fig. 5)~~. At the ZV site, the discrepancy between BW and TBW was primarily driven by the pronounced isotopic contrast between mobile and tightly bound fractions, despite the low proportion of MW in the profile. In contrast, at the TD site, the difference was mainly attributed to a higher proportion of MW, while the isotopic contrast ~~between~~ among the components was less pronounced.

For different~~In cases where~~ BW and TBW~~ differed~~, the average isotopic offset was 0.4~~1~~ ‰ for $\delta^{18}O$ and 2.3~~29~~ ‰ for $\delta^{2}H$, with maximum differences reaching 1.4~~8~~7 ‰ and ~~7.99~~5.2 ‰, respectively. When BW values were used to calculate the SOI, only minimal or no differences between BW and TBW were observed from a broader perspective~~ (Fig. 7)~~. Notable deviations, however, occurred during individual sampling campaigns in April and May. In these instances, the SOI differences between BW and TBW reached up to 0.3.

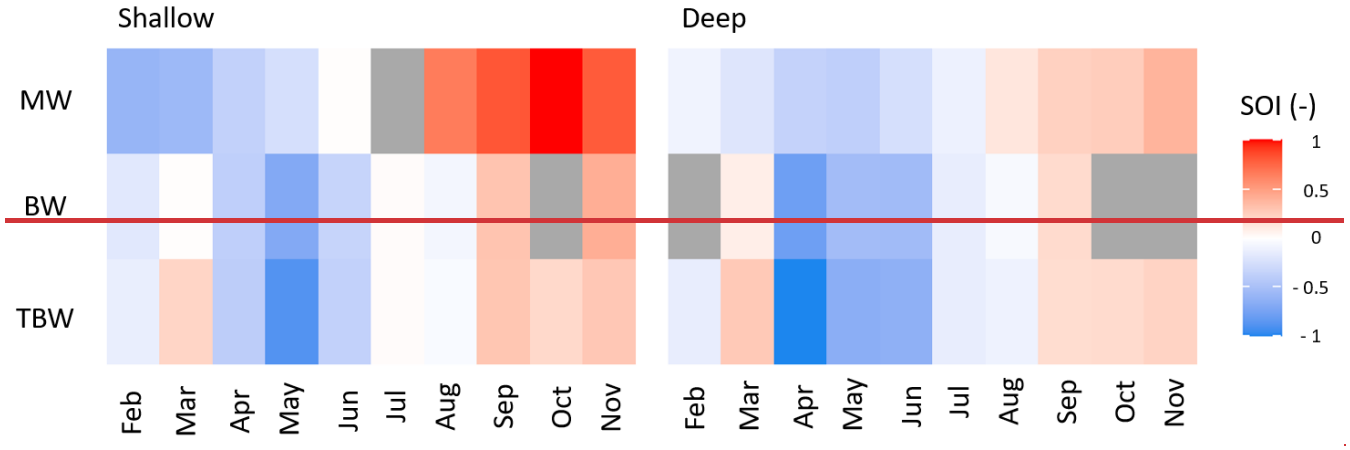

~~**Figure 7.** Comparison of the difference in SOI calculations using mobile (MW), bulk (BW) and tightly bound (TBW) soil water at the Trhové Dušníky site. Values near -1 indicate a predominant contribution from winter precipitation, whereas values approaching 1 reflect a dominant contribution from summer precipitation. Grey areas indicate missing data for the respective period.~~

5 Discussion

5.1 Isotopic changes due to soil properties and precipitation amount

All soil samples obtained in this study fell close to or directly on the LMWL~~, indicating their meteoric origin and suggesting minimal influence of the selected extraction procedures on isotopic composition~~. In ~~C~~consistency~~t~~ with previous studies (e.g., Goldsmith et al., 2012; Hervé-Fernández et al., 2016; Oerter and Bowen, 2017; Sprenger et al., 2018), MW was closely aligned with the LMWL, whereas TBW exhibited a lower slope and greater variability with some samples even outside the 95% precipitation prediction interval. This reflects its longer residence time in the soil profile and indicates the influence of isotopic fractionation associated with evaporation and subsequent condensation and internal mixing processes within the soil matrix (Goldsmith et al., 2012; Sprenger et al., 2016)~~mixing with water of varying ages~~. ~~Interestingly, the isotopic characteristics of TBW in our study were similar to those reported for xylem water in several studies (Oliveira, et al., 2025; Floriancic et al., 2024; Brighenti et al., 2024; Yang et al., 2023; Goldsmith et al., 2019).~~

In agreement with previous studies (e.g., Goldsmith et al., 2012; Geris et al., 2015; Hervé-Fernández et al., 2016; Sprenger et al., 2018), we observed distinct isotopic differences between MW and TBW, particularly in the upper part of the soil profile. These differences decreased with increasing depth, most likely reflecting longer residence times and enhanced mixing within deeper soil layers. Although measurements of cation exchange capacity (CEC) were not available, the very low clay content at all four study sites suggests that isotope fractionation associated with high clay-related CEC (Araguás-Araguás et al., 1995; Meißner et al., 2013; Oerter et al., 2014) was negligible. The observed differences in isotopic composition are therefore more likely attributable to differences in water retention and transport processes between macropores and capillary pore domains.

Despite the occurrence of extreme drought during the sampling year, which should leave an isotopically enriched signal in soil water ~~(Dubbert et al., 2019)~~, no such enrichment was observed at any of the study sites, regardless of precipitation regime or land cover. The reason~~is~~ can be~~was~~ most likely attributed~~due~~ to the sampling depth (20 and 40 cm), as isotopic enrichment from evaporation typically occurs at shallower depths, between 5 and 15 cm (Barnes and Allison, 1988; Sprenger et al., 2017; Oerter and Bowen, 2017; Dubbert et al., 2019). However, while Floriancic et al. (2024) reported no evaporative effect even at 10 cm depth, while other studies (Brooks et al., ~~(~~2010; Sprenger et al., 2016)~~)~~ observed significant evaporative enrichment down to 30 cm. This discrepancy may be ~~attributed~~ caused by the~~o~~ differences in soil texture or extraction methodologies and their associated, often unquantified, errors, particularly under low soil moisture conditions during drought periods (Sprenger et al, 2015; Orlowski et al., 2018).

In agreement with Kleine et al. (2020), we observed a ~~longer mean transit time, inferred from the~~greater phase shift of individual isotopic data~~,~~ in non-forested areas. This phase shift also increased with soil depth, particularly for MW. In contrast, the phase shift observed in TBW remained similar between shallow and deep layers. The greater lag observed in non-forested areas is likely driven by two main factors:

- -PThe first is precipitation amount (Hervé-Fernández et al., 2016) for which higher rainfall can enhance leaching, thereby diminishing the isotopic distinction between MW and TBW.
- -VThe second is vegetation cover as, because, both soil texture and vegetation significantly influence the velocity of the wetting front (Xue et al., 2024).

Preferential flow pathways promote deeper and more rapid infiltration in forested areas, whereas under bare soil or grass, water infiltration proceeds more slowly and diffusively.

The unexpectedly rapid turnover in isotopic composition at our highest-elevation site (RO) contrasts with the results from other studies. For example, Floriancic et al. (2024) reported significant differences in soil water isotopic composition within the top 40 cm, even at forested sites with vegetation cover and precipitation amounts similar to those at our highest-elevation site. These discrepancies may be explained by differences in elevation, mean annual temperature, and soil texture. Lower elevations combined with higher temperatures contribute to acan prolongation of the vegetation growing season, thereby increasing interception and evapotranspiration and reducing the infiltration of precipitation into the soil profile. In addition, the slightly higher silt content at their site likely enhances capillary water retention. Such capillary pores can hold water more effectively and may be bypassed by preferential flow paths, in contrast to the coarse sandy soils at our study sites. This comparison suggests that vegetation cover and soil properties may exert a stronger influence on soil water dynamics than precipitation amount alone.-

5.2 Bulk soil water

Bulk soil water is commonly used as a proxy for the immobile fraction of soil water and is frequently employed in comparisonscompared with xylem water (e. g. Oliveira et al., 2025; Floriancic et al., 2024; Brighenti et al., 2024; Benettin et al., 2024; Barbeta et al., 2019, 2020; Goldsmith et al., 2019; Dubbert et al., 2019; Sprenger et al., 2016). However, the present Our results demonstrate a possible substantial difference that between BW can differ significantly fromand TBW duringat certain periodstimes of the year. Assuming that vegetation may access a less mobile or more tightly bound soil water pool partially disconnected from the mobile water contributing to groundwater recharge and streamflow (Brooks et al., 2010; Goldsmith et al., 2012; McDonell, 2014; Evaristo et al., 2015, 2019), then such differences may introduce uncertainties when identifying the sources of plant xylem water or may lead to an apparent mismatch between BW and xylem water isotopic composition (Oerter and Bowen, 2017; Bowling et al., 2017; Vargas et al., 2017; Barbeta et al., 2019; Lehmann et al., 2025).This isotopic divergence was observed primarily at the onset of the growing season. Following this period, all four study sites experienced substantial drought, which led to progressive drying of the soil profile and a consequent reduction or complete depletion of the MW fraction.

Although the differences observed in our study were most pronounced at the beginning of the growing season, historical data on MW indicate that these differences may vary over time. Some sites exhibit consistent behavior year by year—for example, the site at the highest elevation (RO), where no differences were observed between 2021 and 2023. Here, high total precipitation resulted in an isotopic composition of soil water that closely mirrored that of precipitation each year. In contrast,

at lowland sites (e.g., TD; Fig. 6), MW exhibited a clear phase shift relative to precipitation throughout most of 2022, a year without extreme drought conditions. During the following year, when sampling including TBW was conducted, an extreme summer drought occurred, attenuating this phase shift. These observations suggest that differences between MW and TBW—and consequently between BW and TBW—may occur not only at the beginning of the year but also at other time intervals in dependence on dry or precipitation-rich conditions.~~Historical data of MW from one of the experimental sites (Fig. 8, left), however, indicate that in years without severe drought, isotopic phase shifts within the soil profile, particularly in the MW fraction, can persist throughout the whole year. This persistence may result in subtle but consistent differences between BW and TBW even outside the early spring transition period.~~

Although substituting TBW for BW may result in differences in SOI values of up to approximately 0.3, these differences do not appear to substantially affect the interpretation of long-term isotopic trends across years or study locations. However, this substitution should be considered with caution in short-term or single-event experiments (Lehmann et al., 2025; Muhic et al., 2024; Goldsmith et al., 2012, 2019), particularly under soil and environmental conditions indicating a higher proportion of MW. The high variability of MW can significantly dilute the BW signal and thereby mask the TBW-derived isotopic response.~~Surprisingly, at the highest elevation RO site (where an unexpectedly rapid replacement of water with predominant contribution from winter precipitation was observed), previously collected mobile water data from 2021 to 2023 revealed a consistent pattern (Fig. 8, right), regardless of interannual variability in precipitation and temperature. Assuming that TBW exhibits similar behaviour, the difference between TBW and BW across years is expected to be negligible.~~

~~From a long-term perspective, substituting TBW with BW does not lead to substantially different isotopic interpretations. Furthermore, due to the methodological challenges associated with TBW extraction, this approach is generally unsuitable for routine applications. However, it may be considered in short-term or one-off experiments (e.g., Lehmann et al., 2024), especially when the soil type and environmental conditions indicate a higher proportion of MW. In such cases, isotopic differences can occur – as demonstrated by the 0.3 difference in SOI between BW and TBW – which may result in underestimation of the role of winter precipitation.~~

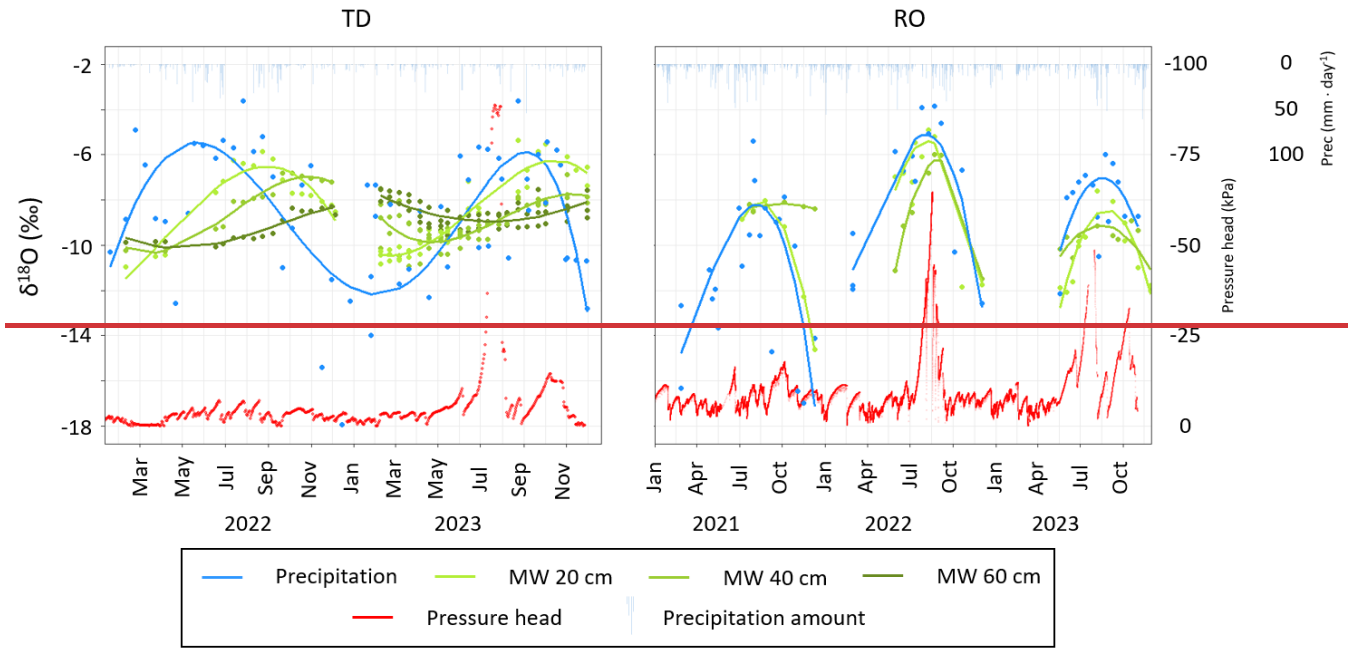
TD
RO
δ18O (‰)
Pressure head (kPa)
Prec (mm · day-1)
Precipitation
MW 20 cm
MW 40 cm
MW 60 cm
Pressure head
Precipitation amount

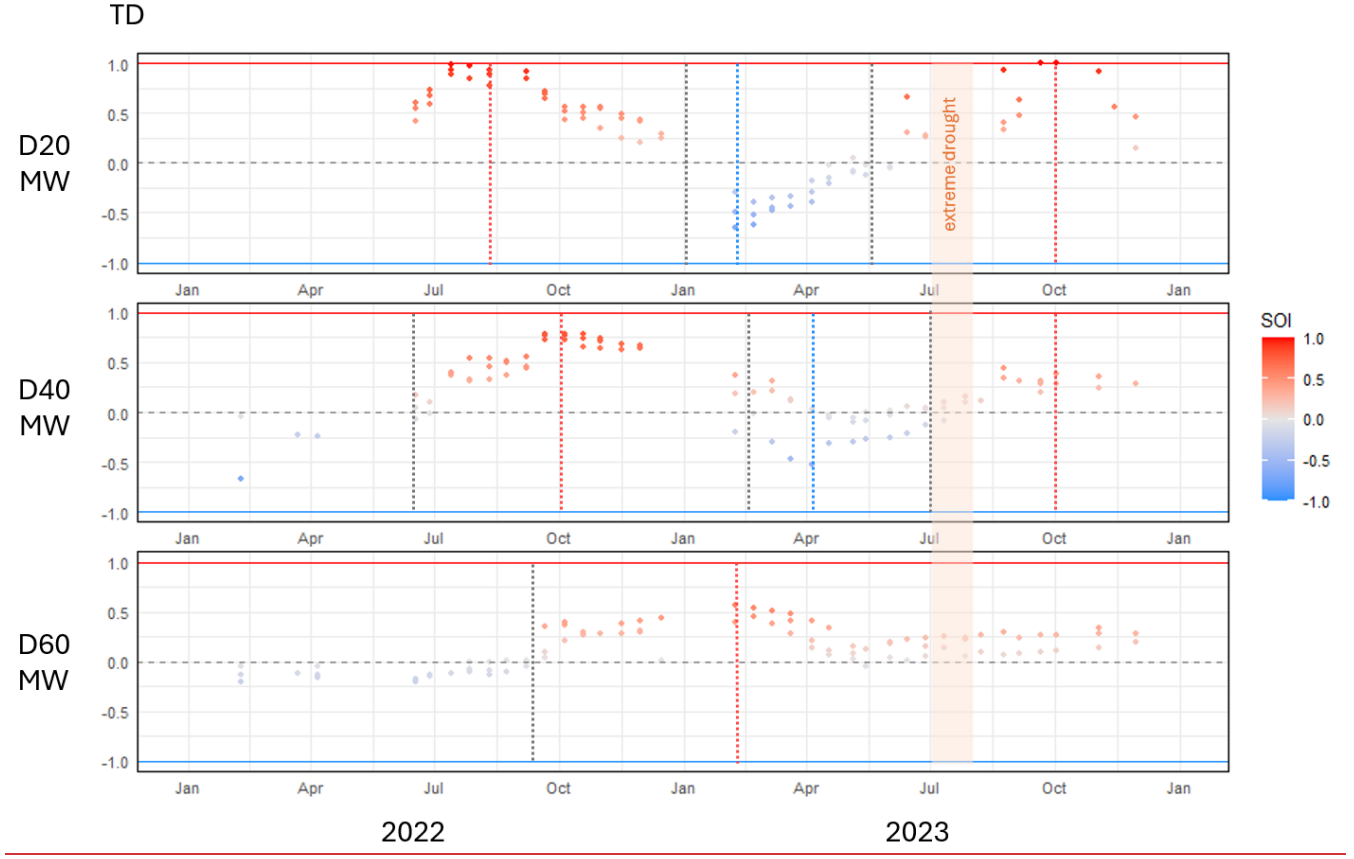
TD
D20 MW
D40 MW
D60 MW
extreme drought
SOI
2022
2023

Figure ~~8~~6. Seasonal origin index (SOI) values of mobile soil water at the TD site at three available depths during 2022–2023. SOI values near −1 indicate a dominant contribution from winter precipitation, whereas values approaching +1 reflect a dominant contribution from summer precipitation. Point colours represent SOI magnitude. The horizontal dashed gray line illustrates the seasonal transition from winter- to summer-dominated precipitation inputs. Vertical dashed lines indicate the timing of maximum dominance of summer (red) and winter (blue) precipitation and their transition (black), highlighting the temporal lag of these events with increasing soil depth.~~Annual cycle of isotopic composition of precipitation (blue) and mobile soil water (shades of green) at the Trhové Dušníky site in 2022–2023 (left) and the Rokytka site in 2021–2023 (right). MW was sampled up to three depths (20, 40, and 60 cm), where darker colour corresponds to greater depths. The red colour represents the suction pressure head at 20 cm depth, and the blue columns at the top of the graph show total precipitation.~~

~~5.3 The importance of winter precipitation~~

~~We hypothesized that winter-derived water would persist longest in soil profiles at higher elevations, where thicker snowpack melts later, compared with lowland areas characterized by transient snow cover and predominantly rainfall-based winter precipitation. This hypothesis was supported by soil water content (SWC) patterns: in lowland sites, SWC remains relatively constant during the first quarter of the year until the onset of the vegetation period or the occurrence of the first dry spells, whereas at higher elevations a distinct snowmelt-induced saturation signal is observed. In the latter case, increasing SWC coincides with gradual snow cover depletion and minimal or absent transpiration, conditions that limit soil moisture loss. Our results show that, with increasing elevation (except at the RO site), the presence of winter-derived water in the soil profile is progressively delayed into later months of the year.~~

~~The above elevation-dependent delay was also evident in the isotopic signatures of various soil water pools. The most rapid response was observed in MW, which exhibited its most isotopically depleted values in lowland sites as early as March, whereas the minimum values in high-elevation sites occurred approximately one month later. This was followed by changes in shallow TBW, with isotopic minima occurring in April in the lowlands and in May at higher elevations. Winter water appeared last in the deeper soil layers (both MW and TBW), with signals emerging from April to May at low elevations and from May to June at the LI site.~~

~~However, at the highest-elevation site, which receives the greatest total precipitation and maintains the most persistent snow cover, we observed, despite limited data and a less pronounced dry season relative to other sites, a consistent pattern in which the isotopic composition of soil water closely mirrors that of precipitation. In this setting, winter water is rapidly displaced from the soil profile by subsequent rainfall events. While isotopically light values of shallow soil water in May and June reflect residual snowmelt, the influence of summer precipitation becomes increasingly evident during the vegetation period. This finding, at least with respect to water in deeper soil layers, contradicts our original hypothesis, which posited that summer precipitation would infiltrate into these layers only during the late summer and autumn months, due to elevated interception and evapotranspiration earlier in the season.~~

5.34 Tightly bound water extraction

To obtain TBW, first the mobile fraction ~~first~~ had to be removed. There are several studies proposing the methods for soil water extraction~~, that tried to extract soil water~~ held in the soil matrix at different tensions (Geris et al., 2019; Bowers et al., 2020; Orlowski et al., 2020). The results of these studies show different isotopic compositions of individual water pools, both with laboratory-prepared (Orlowski et al., 2020; Bowers et al., 2020) and real soil samples (Geris et al., 2015). In this study, we use the pressure plate apparatus, similar to Orlowski et al. (2020), but using~~with~~ a different procedure. In their study, a spike experiment was performed, after which a pressure of 15 bar was applied, and the outflowing water was collected for isotopic analysis. Although labelled water was recovered during a specific time window, the initial and final stages of the experiment yielded water with isotopic signatures differing from the input. This method ~~presents~~ exhibits two basic~~several~~ limitations ~~that~~ hinder~~ing~~ its applicability to natural soil sample~~sples~~:~~.~~

- ~~-T~~~~First, t~~he true isotopic composition of soil water is typically unknown, making it difficult to determine whether the observed isotopic composition already corresponds to soil water. This ambiguity arises from mixing between the soil water and the water used to saturate the ceramic plates within the apparatus, making the collected outflow likely a composite of both sources.
- ~~Second, for the method T~~to ~~be~~ valid~~ate the method~~, every~~ach~~ ceramic plate would have to be conditioned exclusively with samples from a single location and soil depth, to prevent internal mixing of different water sources. This requirement ~~greatly~~ significantly reduces the practicality and scalability of the approach.

In our study, the pressure plate apparatus was employed in a modified configuration. Collected soil samples were subjected to a pressure of 0.6 bar, corresponding to the operational threshold for mobile water typically targeted by field-based suction lysimeters (Brooks et al., 2010; Muñoz-Villers and McDonnell, 2012; Berry et al., 2017; Sprenger et al., 2018; Haagsma et al., 2024). Unlike previous approach~~es~~ that rely on collecting the outflow water (Orlowski et al., 2020), ~~our~~ the presented method involve~~sd~~ a subsequent extraction from pre-dried soil samples. This modification enable~~sd~~ the simultaneous processing of up to 24 samples from various depths and locations within a single run. The subsequent extraction step is conceptually based on isotope mass-balance principles commonly used in hydrology (Haig et al., 2020; Zhao and Wang, 2021; Qiu et al., 2025) or isotopic modelling in general (e.g., Haagsma et al., 2024) and is applied here as an integral part of the extraction procedure itself to reconstruct the isotopic composition of the targeted soil-water fraction.

~~In line with the work of Geris et al. (2015), we observed (until the onset of drought) different isotopic compositions between MW and TBW, especially in the upper part of the profile, with these differences decreasing or disappearing with depth due to longer residence times. Despite the absence of data on cation exchange capacity (CEC), given the very low clay content at all four sites, it can be assumed that fractionation due to high clay CEC (Araguás-Araguás et al., 1995; Meißner et al., 2013; Oerter et al., 2014) was negligible and that differences in isotopic composition were mainly due to different water retention times in macro- and capillary pores.~~

However, ~~To eliminate the influence of the pressure apparatus on the isotopic composition, another potential approach would involve extracting the BW from a subset of samples, while using the pressure plate apparatus on the remaining samples to determine the proportion of MW and TBW. Based on the known isotopic composition of the BW (laboratory extraction) and MW (obtained via suction lysimeters), the isotopic composition of the TBW could then be estimated using the same mixing equation.~~to obtain TBW, we recommend not to use the procedure described in the present study. Instead, the following approach can be recommended:

- Extract MW using standard suction lysimeters,
- Extract BW using each laboratory's standardized procedures (e.g., CVE, DVE-LS),
- apply the mixing equation from this study only for the calculation of TBW, based on the measured isotopic composition of MW and BW and their relative absolute proportions determined gravimetrically (i.e., using a pressure plate apparatus).

This approach allows for the calculation of TBW while removing one procedural step used in this study, thereby reducing error propagation and the uncertainty in the final isotopic composition of TBW.

5.~~4~~5 Data correction

Numerous studies have attempted to compare soil water (including both BW and MW) with xylem water (e.g., Zapater et al., 2011; Meunier et al., 2017; Vargas et al., 2017; Barbeta et al., 2019, 2020; Liu et al., 2021; Lehmann et al., 2025). To enable a meaningful comparison between soil water and xylem water, it is essential to employ an extraction technique ~~that~~ minimizinges isotopic alteration of the sample. However, it is well known that no currently available extraction method can extract soil water from all soil types and moisture contents without introducing some degree of isotopic bias (Sprenger et al., 2015; Orlowski et al., 2018; Kocum et al., 2025).

For this reason, various corrections are often applied to the measured data, although not universally. These include, for instance, adjustments to account for the presence of organic compounds (Martín-Gómez et al., 2015), or corrections based on Rayleigh-type fractionation models (Araguás-Araguás et al., 1995).

~~There is, however,~~ A~~a~~nother important but ~~critical yet~~ frequently overlooked limitation relates to the interpretation of method-validation experiments. N~~While each n~~ewly developed extraction techniques ~~method~~ ate~~is~~ typically tested~~validated~~ using soils of different textures and moisture contents (Dalton, 1988; Revesz and Woods, 1990; Leaney et al., 1993; Scrimgeour, 1995; Wassenaar et al., 2008; Kocum et al., 2025), and the results commonly reveal ~~outcomes of these validation efforts often show a wide range of~~ method-specific offsets expressed as shifts (± SD) relative to the isotopic composition of labelled reference water. ~~inaccuracies.~~ Although t~~T~~hese deviations~~inaccuracies~~ are ~~commonly expressed as the shift ± standard deviation in ‰ from the known isotopic value of labelled water used in the test. Although~~ useful for method comparison, the~~yse~~ are rarely incorporated ~~deviations are generally not applied~~ as corrections into subsequently measured samples~~real measured data~~. To our knowledge, only Yang et al. (2023) explicitly addressed this issue by attempting to account for such method-specific offsets in the interpretation of extracted soil water isotope data.

The correction appliedemployed in this study , which we consider essential for enabling meaningful comparison between individual water samples, relies on conducting spike experiments using the selected chosen extraction method with the site-specific soil types and varying water contents, in our case different dilution rates.. This approach allows us tofor the assessment of the method's performance for specific soil types collected atfrom our study sites. SinceGiven that soil texture and moisture content significantly affectinfluence extraction efficiencyoutcomes (Hendry et al., 2015; Orlowski et al., 2016), such validation experiments should be performed conducted separately for each soil type involved, ideally across a range of moisture conditions in each study. The resulting isotopic deviations (relative to labelled water) should then be incorporated into data correction procedures for actual samples. This condition seems to be essential for enabling meaningful comparison between individual water samples and between laboratories as well, as each CVE setup can differ and yield variable results (Orlowski et al., 2018).

Ultimately, the use of different extraction methods across laboratories, each associated with varying degrees of systematic errors, does not necessarily constitute a critical limitation. The If these methods produce results with low standard deviations, even in the presence of systematic offsets, such biases can be quantified and subsequently corrected. Such calibration should allow meaningful comparisons across studies and research groups.

6 Conclusions

This study demonstrated that soil water stable isotope dynamics vary systematically along an elevational gradient. Despite the absence of snow cover Soil water at lower-elevation at lowland sites with sparse or no snow cover, these areas exhibited longer residence times, whereas high-elevation sites — with substantial winter snow accumulation — showed more rapid isotopic turnover. All soil water samples plotted close to their respective local meteoric water lines, confirming their meteoric origin and indicateding minimal isotopic bias introduced by the applied extraction methods. Mobile soil water most closely mirrored the isotopic composition of precipitation, while tightly bound water, extracted using the newly presented mixing method, reflected showed slight signatures of evaporative enrichment and potential mixing with older water, likely due to its longer residence time in the soil profile and indicated the influence of isotopic fractionation associated with evaporation, subsequent condensation, and internal mixing processes within the soil matrix. Although tightly bound and bulk soil water exhibited only minor isotopic differences on average, seasonal variability increased — particularly in spring and autumn — when differences in isotopic composition and the proportion of mobile to tightly bound water were most pronounced. The largest contrasts between mobile and tightly bound soil water pools occurred during spring and autumn, with maximum differences of 3.3 ‰ and 20.7 ‰ for $\delta^{18}O$ and $\delta^{2}H$, respectively. In such cases, the difference between tightly bound and theoretically calculated bulk soil water reached up to 1.7 ‰ and 5.2 ‰, respectively. These findings highlight the importance of accounting for such variability, especially in short-term or single-time-point studies comparing soil and xylem water for plant source attribution. For such cases, a procedure was proposed to obtain tightly bound soil water. Future research should further explore how these dynamics interact with vegetation type, rooting depth, and changes in precipitation regimes under ongoing climate change.

Code availability. The code is available from the corresponding author upon request.

Data availability. The~~a~~ data that support the findings of~~rom~~ this study are available from the corresponding author upon request.

Author contributions. Concept: JK, LV. Methodology: JK, LV, MS, JHa, OG. Investigation: JK, KF, VS, LV. Formal analysis: JK, JHn, JHa, OG. Resources: VS, MJ, LT, LV. Visualization: JK, KP. Writing (original draft preparation): JK, KF, VS. Writing (review and editing): JK, KF, VS, KP, JHa, OG, JHn, MJ, MS, LT, LV. Supervision: LV.

Competing interests. The authors declare that they have no conflict of interest.

Acknowledgements. The authors warmly thank David Pěsta for assistance with soil sampling.

Financial support. This work was supported by the Czech Academy of Sciences (grant no. RVO 67985874), the research programme Strategy AV21 Water for Life, the Czech Science Foundation (grant no. GA CR 23-06859K), and the Faculty of Science of Charles University in Prague (grant no. SVV 244-2606941).

References

Allen, S. T., Kirchner, J. W., Braun, S., Siegwolf, R. T. W., and Goldsmith, G. R.: Seasonal origins of soil water used by trees, Hydrology and Earth System Sciences, 23, 1199–1210, https://doi.org/10.5194/hess-23-1199-2019, 2019.

Araguás-Araguás, L., Rozanski, K., Gonfiantini, R., and Louvat, D.: Isotope effects accompanying vacuum extraction of soil water for stable isotope analyses, Journal of Hydrology, 168, 159–171, https://doi.org/10.1016/0022-1694(94)02636-P, 1995.

Barbeta, A., Gimeno, T. E., Clavé, L., Fréjaville, B., Jones, S. P., Delvigne, C., Wingate, L., and Ogée, J.: An explanation for the isotopic offset between soil and stem water in a temperate tree species, New Phytologist, 227, 766–779, https://doi.org/10.1111/nph.16564, 2020.

Barbeta, A., Jones, S. P., Clavé, L., Gimeno, T. E., Fréjaville, B., Wohl, S., and Ogée, J.: Unexplained hydrogen isotope offset complicate the identification and quantification of tree water sources in a riparian forest. Hydrology and Earth System Sciences, 23, 2129–2146, https://doi.org/10.5194/hess-23-2129-2019, 2019.

Barnes, C. J., and Allison, G. B.: Tracing of water movement in the unsaturated zone using stable isotopes of hydrogen and oxygen, Journal of Hydrology, 100, 143–176, https://doi.org/10.1016/0022-1694(88)90184-9, 1988.

Bates, C. G.: First results in the streamflow experiment, Wagon Wheel Gap, Colorado, Journal of Forestry, 19, 402–408, 1921.

Benettin, P., Tagliavini, M., Adreotti, C., di Villahermosa F. S. M., Verdone, M., Dani, A., and Penna, D.: Ecohydrological Dynamics and Temporal Water Origin in a European Mediterranean Vineyard, Ecohydrology, 18, e2711, https://doi.org/10.1002/eco.2711, 2024.

Benettin, P., Volkmann, T. H. M., von Freyberg, J., Frentress, J., Penna, D., Dawson, T. E., and Kirchner, J. W.: Effects of climatic seasonality on the isotopic composition of evaporating soil waters, Hydrology and Earth System Sciences, 22, 288–2890, https://doi.org/10.5194/hess-22-2881-2018, 2018.

Berry, Z. C., Evaristo, J., Moore, G., Poca, M., Steppe, K., Verrot, L., Asbjornsen, H., Borma, L. S., Bretfeld, M., Hervé-Fernández, P., Seyfried, M., Schwendenmann, L., Sinacore, K., De Wispelaere, L., and McDonell, J. J.: The two water worlds hypothesis: Addressing multiple working hypotheses and proposing a way forward, Ecohydrology, 11, e1843, https://doi.org/10.1002/eco.1843, 2017.

Bond, B. J., Jones, J. A., Moore, G., Phillips, N., Post, D., and McDonell, J. J.: The zone of vegetation influence on baseflow revealed by diel patterns of streamflow and vegetation water use in a headwater basin, Hydrological Processes, 16, 1671–1677, https://doi.org/10.1002/hyp.5022, 2002.

Bowers, W. H., Mercer, J. J., Pleasants, M. S., and Williams, D. G.: A combination of soil water extraction methods quantifies the isotopic mixing of waters held at separate tensions in soil, Hydrology and Earth System Sciences, 24, 4045–4060, https://doi.org/10.5194/hess-24-4045-2020, 2020.

Bowling, D. R., Schulze, E. S., and Hall, S. J.: Revisiting streamside trees that do not use stream water: can the two water worlds hypothesis and snowpack isotopic effects explain a missing water source?, Ecohydrology, 10, e1771, https://doi.org/10.1002/eco.1771, 2017.

Brighenti, S., Obojes, N., Bertoldi, G., Zuecco, G., Censini, M., Cassiani, G., Penna, D., and Francesco, C.: Snowmelt and subsurface heterogeneity control tree water sources in a subalpine forest, Ecohydrology, 17, e2695, https://doi.org/10.1002/eco.2695, 2024.

Brooks, J., Barnard, H., Coulombe, R., and McDonell, J. J.: Ecohydrologic separation of water between trees and streams in a Mediterranean climate, Nature Geoscience, 3, 100–104, https://doi.org/10.1038/ngeo722, 2010.

Büntgen, U., Urban, O., Krusic, P. J., Rybníček, M., Kolář, T., Kyncl, T., Ač, A., Koňasová, E., Čáslavský, J., Esper, J., Wagner, S., Saurer, M., Tegel, W., Dobrovolný, P., Cherubini, P., Reining, F., and Trnka, M.: Recent European drought extremes beyond Common Era background variability, Nature Geoscience, 14, 190–196, https://doi.org/10.1038/s41561-021-00698-0, 2021.

~~Ceperley, N., Gimeno, T. E., Jacobs, S. R., Beyer, M., Dubbert, M., Fischer, B., Geris, J., Holko, L., Kübert, A., Le Gall, S., Lehmann, M. M., Llorens, P., Millar, C., Penna, D., Prieto, I., Radolinski, J., Scandellari, F., Stockinger, M., Stumpp, C., Tetzlaff, D., van Meerveld, I., Werner, C., Yildiz, O., Zuecco, G., Barbeta, A., Orlowski, N., and Rothfuss, Y.: Toward a common methodological framework for the sampling, extraction, and isotopic analysis of water in the Critical Zone to study vegetation water use, WIREs Water, 11, e1727, https://doi.org/10.1002/wat2.1727, 2024.~~

Craig, H.: Standard for reporting concentrations of deuterium and oxygen-18 in natural waters, Science, 133, 1833–1834, https://doi.org/10.1126/science.133.3467.1833, 1961.

Dalton, F. N.: Plant root water extraction studies using stable isotopes, Plant Soil, 111, 217–221, https://doi.org/10.1007/BF02139942, 1988.

Davison, A. C., and Hinkley, D. V.: Bootstrap Methods and their Application, Cambridge University Press, Cambridge, United Kingdom, https://doi.org/10.1017/CBO9780511802843, 1997.

Dawson, T. E., and Ehleringer, J. R.: Streamside trees that do not use stream water, Nature, 350, 335–337, https://doi.org/10.1038/350335a0, 1991.

Dubbert, M., Caldeira, M. C., Dubbert, D., and Werner, C.: A pool-weighted perspective on the two-water-worlds hypothesis, New Phytologist, 222, 1271–1283, https://doi.org/10.1111/nph.15670, 2019.

Evaristo, J., Kim, M., van Haren, J., Pangle, L. A., Harman, C. J., Troch, P. A., and McDonell, J. J.: Characterizing the fluxes and age distribution of soil water, plant water and deep percolation in a model tropical ecosystem, Water Resources Research, 55, 3307–3327, https://doi.org/10.1029/2018WR023265, 2019.

Evaristo, J., Jasechko, S., and McDonell, J. J.: Global separation of plant transpiration from groundwater and streamflow, Nature, 525, 91–94, https://doi.org/10.1038/nature14983, 2015.

Floriancic, M. G., Allen, S. T. and Kirchner, J. W.: Isotopic evidence for seasonal water sources in tree xylem and forest soils, Ecohydrology, 17, e2641, https://doi.org/10.1002/eco.2641, 2024.

Gebrechorkos, S. H., Sheffield, J., Vicente-Serrano, S. M., Funk, C., Miralles, D. G., Peng, J., Dyer, E., Talib, J., Beck, H. E., Singer, M. B., and Dadson, S. J.: Warming accelerates global drought severity, Nature, 642, 628–635, https://doi.org/10.1038/s41586-025-09047-2, 2025.

Geris, J., Tetzlaff, D., McDonell, J. J., Anderson, J., Paton, G., and Soulsby, C.: Ecohydrological separation in wet, low energy northern environments? A preliminary assessment using different soil water extraction techniques, Hydrological Processes, 15, 5139–5152, https://doi.org/10.1002/hyp.10603, 2015.

Goldsmith, G., Allen, S., Braun, S., Engbersen, N., González-Quijano, C. R., Kirchner, J. W., and Siegwolf, R. T. W.: Spatial variation in throughfall, soil, and plant water isotopes in a temperate forest, Ecohydrology, 12, 1–11, https://doi.org/10.1002/eco.2059, 2019.

Goldsmith, G. R., Muñoz-Villers, L. E., Holwerda, F., McDonell, J. J., Asbjornsen, H., and Dawson, T. E.: Stable isotopes reveal linkages among ecohydrological processes in a seasonally dry tropical montane cloud forest, Ecohydrology, 5, 779–790, https://doi.org/10.1002/eco.268, 2012.

Gradmann, H.: Untersuchungen über die Wasserverhältnisse des Bodens als Grundlage des Pflanzenwachstums, Jahrbücher für wissenschaftliche Botanik, 69,1-100, 1928.

Haagsma, M., Finkenbiner, C. E., None, D. C., Bowen, G. J., Still, C., Fiorella, R. P., and Good, S. P.: Using an Isotope Enabled Mass Balance to Evaluate Existing Land Surface Models, Water Resources Research, 60, e2024WR037530, https://doi.org/10.1029/2024WR037530, 2024.

Hackmann, C. A., Paligi, S. S., Mund, M., Hölscher, D., Leuschner, C., Pietig, K., and Ammer, C.: Root water uptake depth in temperate forest trees: species-specific patterns shaped by neighbourhood and environment, Plant biology, Advance online publication, https://doi.org/10.1111/plb.70058, 2025.

Haig, H. A., Hayes, N. M., Simpson, G. L., Yi, Y., Wissel, B., Hodder, K. R., and Leavitt, P. R.: Comparison of isotopic mass balance and instrumental techniques as estimates of basin hydrology in seven connected lakes over 12 years, Journal of Hydrology, 6, 100046, https://doi.org/10.1016/j.hydroa.2019.100046, 2020.

Harper, W. V.: Reduced Major Axis Regression: Teaching Alternatives to Least Squares, Wiley StatsRef: Statistics Reference Online, https://doi.org/10.1002/9781118445112.stat07912, 2016.

Harpold, A. A., Kaplan, M. L., Klos, P. Z., Link, T., McNamara, J. P., Rajagopal, S., Schumer, R., and Steele, C. M.: Rain or snow: hydrologic processes, observations, prediction, and research needs, Hydrology and Earth System Sciences, 21, 1–22, https://doi.org/10.5194/hess-21-1-2017, 2017.

Hendry, M. J., Schmeling, E., Wassenaar, L. I., Barbour, S. L., Pratt, D.: Determining the stable isotope composition of pore water from saturated and unsaturated zone core: improvements to the direct vapour equilibration laser spectrometry method, Hydrology and Earth System Sciences, 19, 4427–4440, https://doi:10.5194/hess-19-4427-2015, 2015.

Hervé-Fernández, P., Oyarzún, C., Brumbt, C., Bodé, H. S., Verhoest, N. E. C., and Boeckx, P.: Assessing the 'two water worlds' hypothesis and water sources for native and exotic evergreen species in south central Chile, Hydrological Processes, 15, 4227–4241, https://doi.org/10.1002/hyp.10984, 2016.

Jenicek, M., Hnilica, J., Nedelcev, O., Sipek, V.: Future changes in snowpack will impact seasonal runoff and low flows in Czechia, Journal of Hydrology: Regional Studies, 37, 100899, https://doi.org/10.1016/j.ejrh.2021.100899, 2021.

Jenicek, M., and Ledvinka, O.: Importance of snowmelt contribution to seasonal runoff and summer low flows in Czechia, Hydrology and Earth System Sciences, 24, 3475–3491, https://doi.org/10.5194/hess-24-3475-2020, 2020.

Jenicek, M., Seibert, J., and Staudinger, M.: Modeling of Future Changes in Seasonal Snowpack and Impacts on Summer Low Flows in Alpine Catchments, Water Resources Research, 54, 538–556, https://doi.org/10.1002/2017WR021648, 2018.

Jiao, W., Wang, L., Smith, W. K., Chang, Q., Wang, H., and D'Odorico, P.: Observed increasing water constraint on vegetation growth over the last three decades, Nature Communication, 12, 3777, https://doi.org/10.1038/s41467-021-024016-9, 2021.

Kirchner, J. W.: Aggregation in environmental systems – Part 1: Seasonal tracer cycles quantify young water fractions, but not mean transit times, in spatially heterogeneous catchments, Hydrology and Earth System Sciences, 20, 279–297, https://doi.org/10.5194/hess-20-279-2016, 2016.

Kleine, L., Tetzlaff, D., Smith, A., Wang, H., and Soulsby, C.: Using water stable isotopes to understand evaporation, moisture stress, and re-wetting in catchment forest and grassland soils of the summer drought of 2018, Hydrology and Earth System Sciences, 24, 3737–3752, https://doi.org/10.5194/hess-24-3737-2020, 2020.

Kocum, J., Haidl, J., Gebousky, O., Falatkova, K., Sipek, V., Sanda, M., Orlowski, N., and Vlcek, L.: Technical note: A new laboratory approach to extract soil water for stable isotope analysis from large soil samples, Hydrology and Earth System Sciences, 29, 2863–2880, https://doi.org/10.5194/hess-29-2863-2025, 2025.

Landwehr, J. M., and Coplen, T. B.: Line-condition excess: A new method for characterizing stable hydrogen and oxygen isotope ratios in hydrologic systems, Isotopes in Environmental Studies, Edition: 1, IAEA, ISBN: 92-0-111305-X, 2006.

Leaney, F. W., Smettem, K. R. J., and Chittleborough, D. J.: Estimating the contribution of preferential flow to subsurface runoff from a hillslope using deuterium and chloride, Journal of Hydrology, 147, 83–103, https://doi.org/10.1016/0022-1694(93)90076-L, 1993.

Lehmann, M. M., Geris, J., van Meerveld, I., Penna, D., Rothfuss, Y., Verdone, M., Ala-Aho, P., Arvai, M., Babre, ~~M. A.~~ A., Balandier, P., Bernhard, F., Butorac, L., Carrière, S. D., Ceperley, N. C., Chen, Z., Correa, A., Diao, H., Dubbert, D., Dubbert, M., Ercoli, F., Floriancic, M. G., Ghazoul, A., Gimeno, T. E., Gounelle, D., Hagedorn, F., Hissler, C., Huneau, F., Iraheta, A., Jakovljević, T., Kazakis, N., Kern, Z., Kinzinger, L., Knaebel, K., Kobler, J., Kocum, J., Koeber, C., Koren, G., Kübert, A., Kupka, D., Le Gall, S., Lehtonen, A., Leydier, T., Malagoli, P., Manca di Villahermosa, F. S., Marchina, C., Martínez-Carreras, N., Martin-StPaul, N., Marttila, H., Oliveira, A. M., Monvoisin, G., Orlowski, N., Palmik-Das, K., Persoiu, A., Popa, A., Prikaziuk, E., Quantin, C., Rinne-Garmston, K. T., Rohde, C., Sanda, M., Saurer, M., Schulz, D., Stockinger, M. P., Stumpp, C., Venisse, J. S., Vlcek, L., Voudouris, S., Weeser, B., Wilkinson, M. E., Zuecco, G., and Meusburger, K.: Soil and tree stem xylem water isotope data from two pan-European sampling campaigns, Earth System Science Data, 17, 6129–6147~~[preprint]~~, https://doi.org/10.5194/essd-17-6129-2025~~https://doi.org/10.5194/essd-2024-409, in review~~, 20254.

Liu, J., Si, Z., Wu, L., Chen, J., Gao, Y., and Duan, A.: Using stable isotopes to quantify root water uptake under a new planting pattern of high-low seed beds cultivation in winter wheat, Soil and Tillage Research, 205, 104816, https://doi.org/10.1016/j.still.2020.104816, 2021.

Mankin, J. S., Seager, R., Smerdon, J. E., Cook, B. I., and Williams, A. P.: Mid-latitude freshwater availability reduced by projected vegetation responses to climate change, Nature Geoscience, 12, 983–988, https://doi.org/10.1038/s41561-019-0480-x, 2019.

Martín-Gómez, P., Barbeta, A., Voltas, J., Peñuelas, J., Dennis, K., Palacio, S., Dawson, T. E., and Ferrio, J. P.: Isotope-ratio infrared spectroscopy: a reliable tool for the investigation of plant-water sources?, New Phytologist, 207, 914–927, https://doi.org/10.1111/nph.13376, 2015.

Marty, C., Tilg, A. M., and Jonas, T.: Recent Evidence of Large-Scale Receding Snow Water Equivalents in the European Alps, Journal of Hydrometeorology, 18, 1021–1031, https://doi.org/10.1175/JHM-D-16-0188.1, 2017.

McDonell, J. J.: The two water worlds hypothesis: ecohydrological separation of water between streams and trees?, WIREs Water, 1, 323–329, https://doi.org/10.1002/wat2.1027, 2014.

Meißner, M., Köhler, M., Schwendenmann, L., Hölscher, D., and Dyckmans, J.: Soil water uptake by trees using water stable isotopes (δ^2H and $\delta^{18}O$)-a method test regarding soil moisture, texture and carbonate, Plant Soil, 376, 327–335, https://doi.org/10.1007/s11104-013-1970-z, 2024.

Meunier, F., Rothfuss, Y., Bariac, T., Biron, P., Richard, P., Durand, J. L., Couvreur, V., Vanderborght, J., and Javaux, M.: Measuring and Modeling Hydraulic Lift of *Lolium multiflorum* Using Stable Water Isotopes, Vadose Zone Journal, 17, 1–15, https://doi.org/10.2136/vzj2016.12.0134, 2017.

Molz, J. F.: Models of water transport in the soil-plant system: A review, Water Resources Research, 17, 1245–1260, https://doi.org/10.1029/WR017i005p01245, 1981.

Muhic, F., Ala-Aho, P., Sprenger, M., Klöve, B., and Hannu Marttila.: Snowmelt-mediated isotopic homogenization of shallow till soil, Hydrology and Earth System Sciences, 28, 4861–4881, https://doi.org/10.5194/hess-28-4861-2024, 2024.

Muñoz-Villers, L. E., and McDonell, J. J.: Runoff generation in a steep, tropical montane cloud forest catchment on permeable volcanic substrate, Water Resources Research, 48, https://doi.org/10.1029/2011WR011316, 2012.

Musselmann, K. N., Clark, M. P., Liu, C., Ikeda, K., and Rasmussen, R.: Slower snowmelt in a warmer world, Nature Climate Change, 7, 214–219, https://doi.org/10.1038/nclimate3225, 2017.

Oerter, E., J., and Bowen, G.: Spatio-temporal heterogeneity in soil water stable isotopic composition and its ecohydrologic implications in semiarid ecosystems, Hydrological Processes, 33, 1724–1738, https://doi.org/10.1002/hyp.13434, 2019.

Oerter, E. J., and Bowen, G.: In situ monitoring of H and O stable isotopes in soil water reveals ecohydrologic dynamics in managed soil systems, Ecohydrology, 10, e1841, https://doi.org/10.1002/eco.1841, 2017.

Oerter, E., Finstad, K., Schaefer, J., Goldsmith, G. R., Dawson, T., and Amundson, R.: Oxygen isotope fractionation effects in soil water via interaction with cations (Mg, Ca, K, Na) adsorbed to phyllosilicate clay minerals, Journal of Hydrology, 515, 1–9, https://doi.org/10.1016/j.jhydrol.2014.04.029, 2014.

Oliveira, A. M., Floriancic, M., Gianasi, F. M., Herbstritt, B., Pompeu, P. V., Araújo, F. C., Silva-Sene, A. M., Reis, M. G., Farrapo, C. L., Ferreira, L. A. S., dos Santos, R. M., and van Meerveld, I.: Isotopic Composition of Soil and Xylem Water Across Six Seasonal Floodplain Forests in Southeastern Brazil, Ecohydrology, 18, e70076, https://doi.org/10.1002/eco.70076, 2025.

Orlowski, N., and Breuer, L.: Sampling soil water along pF curve for $\delta^{2}H$ and $\delta^{18}O$ analysis, Hydrological Processes, 34, 4959–4972, https://doi.org/10.1002/hyp.13916, 2020.

Orlowski, N., Breuer, L., Angeli, N., Boeckx, P., Brumbt, C., Cook, C. S., Dubbert, M., Dyckmans, J., Gallagher, B., Gralher, B., Herbstritt, B., Hervé-Fernández, P., Hissler, C., Koeniger, P., Legout, A., Macdonald, C. J., Oyarzún, C., Redelstein, R., Seidler, C., Siegwolf, R., Stumpp, C., Thomsen, S., Weiler, M., Werner, C., and McDonnell, J. J.: Inter-laboratory comparison of cryogenic water extraction systems for stable isotope analysis of soil water, Hydrology and Earth System Sciences, 22, 3619–3637, https://doi.org/10.5194/hess-22-3619-2018, 2018.

Orlowski, N., Breuer, L., and McDonell, J. J.: Critical issues with cryogenic extraction of soil water for stable isotope analysis, Ecohydrology, 9, 3–10, https://doi.org/10.1002/eco.1722, 2016.

Qin, Y., Abatzoglou, J. T., Siebert, S., Huning, L. S., AghaKouchak, A., Mankin, J. S., Hong, C., Tong, D., Davis, S. J., and Mueller, N. D.: Agricultural risks from changing snowmelt, Nature Climate Change, 10, 459–465, https://doi.org/10.1038/s41558-020-0746-8, 2020.

Qiu, X., Zhang, M., Wang, S., Meng, H., and Che, C.: Comparison of stable isotope mixing models for examining plant root water uptake, PLOS ONE, 20, e0318771, https://doi.org/10.1371/journal.pone.0318771, 2025.

Revesz, K., and Woods, P. H.: A method to extract soil water for stable isotope analysis, Journal of Hydrology, 115, 397–406, https://doi.org/10.1016/0022-1694(90)90217-L, 1990.

Safeeq, M., Shukla, S., Arismendi, I., Grant, G. E., Lewis, S. L., and Nolin, A.: Influence of winter season climate variability on snow-precipitation ratio in the western United States, International Journal of Climatology, 36, 3175–3190, https://doi.org/10.1002/joc.4545, 2015.

Samaniego, L., Thober, S., Kumar, R., Wanders, N., Rakovec, O., Pan, M., Zink, M., Sheffield, J., Wood, E. F., and Marx, A.: Anthropogenic warming exacerbates European soil moisture droughts, Nature Climate Change, 8, 421–426, https://doi.org/10.1038/s41558-018-0138-5, 2018.

Scrimgeour, C. M.: Measurement of plant and soil water isotope composition by direct equilibration methods, Journal of Hydrology, 172, 261–274, https://doi.org/10.1016/0022-1694(95)02716-3, 1995.

Seyedsadr, S., Šípek, V., Jačka, L., Sněhota, M., Beesley, L., Pohořelý, M., Kovář, M., and Trakal, L.: Biochar considerably increases the easily available water and nutrient content in low-organic soils amended with compost and manure, Chemosphere, 293, 133586, https://doi.org/10.1016/j.chemosphere.2022.133586, 2022.

Šípek, V., Jenicek, M., Hnilica, J., and Zelíková, N.: Catchment Storage and its Influence on Summer Low Flows in Central European Mountainous Catchments, Water Resources Management, 35, 2829–2843, https://doi.org/10.1007/s11269-021-02871-x, 2021.

Šípek, V., Jačka, L., Seyedsadr, S., and Trakal, L.: Manifestation of spatial and temporal variability of soil hydraulic properties in the uncultivated Fluvisol and performance of hydrological model, Catena, 182, 104119, https://doi.org/10.1016/j.catena.2019.104119, 2019.

Sprenger, M., Tetzlaff, D., Buttle, J., Laudon, H., Leistert, H., Mitchell, C. P. J., Snelgrove, J., Weiler, M., and Soulsby, C.: Measuring and Modeling Stable Isotopes of Mobile and Bulk Soil Water, Vadose Zone Journal, 17, 1–18, https://doi.org/10.2136/vzj2017.08.0149, 2018.

Sprenger, M., Tetzlaff, D., and Soulsby, C.: Soil water stable isotopes reveal evaporation dynamics at the soil–plant–atmosphere interface of the critical zone, Hydrology and Earth System Sciences, 21, 3839–3858, https://doi.org/10.5194/hess-21-3839-2017, 2017.

Sprenger, M., Leistert, H. Gumbel, K., and Weiler, M.: Illuminating hydrological processes at the soil-vegetation-atmosphere interface with water stable isotopes, Reviews of Geophysics, 54, 674–704, https://doi.org/10.1002/2015RG000515, 2016.

Sprenger, M., Herbstritt, B., and Weiler, M.: Established methods and new opportunities for pore water stable isotope analysis, Hydrological Processes, 29, 5174–5192, https://doi.org/10.1002/hyp.10643, 2015.

Tinker, P. B.: Transport of water to plant root in soil, Philosophical Transactions of the Royal Society of London, 273, 445–461, https://doi.org/10.1098/rstb.1976.0024, 1976.

Tolasz, R., Míková, T., Valeriánová, A., and Voženílek, V.: Climate atlas of Czechia. 1. vyd., 255s., Praha: Český hydrometeorologický ústav; Olomouc: Univerzita Palackého v Olomouci. ISBN: 978-80-86690-26-1, 2007.

van den Honert, T. H.: Water transport in plats as a catenary process, Discussions of the Faraday Society, 3, 146–153, https://doi.org/10.1039/DF9480300146, 1948.

Vargas, A. I., Schaffer, B., Yuhong, L., and Sternberg, L. S. L.: Testing plant use of mobile vs immobile soil water sources using stable isotope experiments, New Phytologist, 215, 582–594, https://doi.org/10.1111/nph.14616, 2017.

Vlček, L., Šípek, V., Kofroňová, J., Kocum, J., Doležal, T., and Janský, B.: Runoff formation in a catchment with Peat bog and Podzol hillslopes, Journal of Hydrology, 593, 125633, https://doi.org/10.1016/j.jhydrol.2020.125633, 2021.

Wassenaar, L. I., Hendry, M. J., Chostner, V. L., and Lis, G. P.: High Resolution Pore Water δ^2H and $\delta^{18}O$ Measurements by $H_2O_{(liquid)}$-$H_2O_{(vapor)}$ Equilibration Laser Spectroscopy, Environmental Science & Technology, 42, 9262–9267, https://doi.org/10.1021/es802065s, 2008.

Weatherley, P. E.: Introduction: Water movement through plants, Philosophical Transactions of the Royal Society of London, 273, 435–444, https://doi.org/10.1098/rstb.1976.0023, 1976.

Willibald, F., Kotlarski, S., Grêt-Regamey, A., and Ludwig, R.: Anthropogenic climate change versus internal climate variability: impacts on snow cover in the Swiss Alps, The Cryosphere, 14, 2909–2924, https://doi.org/10.5194/tc-14-2909-2020, 2020.

Xia, C., Zuecco, G., Marchina, C., Penna, D., and Borga, M.: Effects of Short-Term Climate Variations on Young Water Fraction in a Small Pre-Alpine Catchment, Water Resources Research, 60, e2023WR036245, https://doi.org/10.1029/2023WR036245, 2024.

Xue, D., Tian, J., Zhang, B., Kang, W., Zhou, Y., and He, C.: Effects of vegetation types on soil wetting pattern and preferential flow in arid mountainous areas of northwest China, Journal of Hydrology, 642, 131849, https://doi.org/10.1016/j.jhydrol.2024.131849, 2024.

Yang, B., Dossa, G. G. O., Hu, Y. H., Liu, L. L., Meng, X. J., Du, Y. Y., Li, J. Y., Zhu, X. A., Zhang, Y. J., Singh, A. K., Yuan, X., Wu, J. E., Zakari, S., Liu, W. J., and Song, L.: Uncorrected soil water isotopes through cryogenic vacuum distillation may lead to a false estimation on plant water sources, Methods in Evology and Evolution, 14, 1443–1456, https://doi.org/10.1111/2041-210X.14107, 2023.

Zapater, M., Hossann, C., Bréda, N., Bréchet, C., Bonal, D., and Granier, A.: Evidence of hydraulic lift in a young beech and oak mixed forest using ^{18}O soil water labelling, Trees, 25, 885–894, https://doi.org/10.1007/s00468-011-0563-9, 2011.

Zelíková, N., Toušková, J., Kocum, J., Vlček, L., Tesař, M., Bouda, M., and Šípek, V.: Divergent water balance trajectories under two dominant tree species in montane forest catchment shifting from energy- to water-limitation, Hydrology and Earth System Sciences, 29, 6003–6021~~[preprint]~~, https://doi.org/10.5194/hess-29-6003-2025~~https://doi.org/10.5194/hess-2024-244, in review~~, 2025.

Zhao, Y., and Wang, L.: Insights into the isotopic mismatch between bulk soil water and *Salix matsudana* Koidz trunk water from root water stable isotope measurements, Hydrology and Earth System Sciences, 25, 3975–3989, https://doi.org/10.5194/hess-25-3975-2021, 2021.